Precambrian Research 176 (2010) 46–64

Contents lists available at ScienceDirect

Precambrian Research

journal homepage: www.elsevier.com/locate/precamres

The Ediacaran radiogenic Sr isotope excursion in the Doushantuo Formation in the Three Gorges area, South China

Yusuke Sawaki[a,*], Takeshi Ohno[a,b], Miyuki Tahata[a], Tsuyoshi Komiya[a,b], Takafumi Hirata[a,b], Shigenori Maruyama[a,b], Brian F. Windley[c], Jian Han[d], Degan Shu[d], Yong Li[e]

[a] Department of Earth and Planetary Sciences, Tokyo Institute of Technology, 2-12-1 Ookayama, Meguro-ku, Tokyo 152-8551, Japan
[b] Research Center for the Evolving Earth and Planets, Tokyo Institute of Technology, 2-12-1 Ookayama, Meguro-ku, Tokyo 152-8551, Japan
[c] Department of Geology, The University of Leicester, Leicester LE1 7RH, UK
[d] Department of Geology and Key Laboratory for Continental Dynamics, Northwest University, Xi'an 710069, China
[e] School of Earth Sciences and Resources, Chang'an University, Xi'an 710054, China

ARTICLE INFO

Article history:
Received 13 February 2009
Received in revised form 11 October 2009
Accepted 24 October 2009

Keywords:
Neoproterozoic
Multiple isotope systems of $^{87}Sr/^{86}Sr$
$^{88}Sr/^{86}Sr$
$\delta^{13}C$ and $\delta^{18}O$
Doushantuo Formation
Biological evolution
Nutrients
Gaskiers glaciation
Gondwana supercontinent
Shuram excursion

ABSTRACT

The Ediacaran period was one of the most important times for the evolution of life. However, the scarcity of well-preserved outcrops of Ediacaran rocks still leaves ambiguity in decoding ambient surface environmental changes and biological evolution.

The Ediacaran strata in South China are almost continuously exposed, comprise mainly carbonate rocks with subordinate black shales and sandstones, and they contain many fossils, suitable for study of environmental and biological changes in the Ediacaran. We conducted drilling through the Doushantuo Fm at four sites in the Three Gorges area to obtain continuous, fresh samples without surface alteration and oxidation. We analyzed $^{87}Sr/^{86}Sr$ and $^{88}Sr/^{86}Sr$ ratios of the fresh carbonate rocks, selected on the basis of microscopic observations and the geochemical signatures of Sr contents, Mn/Sr and Rb/Sr ratios, and $\delta^{18}O$ values, with a multiple collector-inductively coupled plasma-mass spectrometer (MC-ICP-MS).

The chemostratigraphy of the $^{87}Sr/^{86}Sr$ ratios of the drilled samples displays a smooth curve and two large positive shifts during Ediacaran time. The combination of the detailed chemostratigraphies of $\delta^{13}C$, $\delta^{18}O$ and $^{87}Sr/^{86}Sr$ values and Mn and Fe contents enables us to decode the surface environmental changes and their causes in the Ediacaran. The first large positive excursion of $^{87}Sr/^{86}Sr$ occurred together with negative $\delta^{13}C$ and positive $\delta^{18}O$ excursions. The higher $^{87}Sr/^{86}Sr$ values indicate an enhancement of continental weathering, whereas the positive $\delta^{18}O$ excursion suggests global cooling. Global regression due to global cooling enhanced the oxidative decay of exposed marine organic sediments and continental weathering. Accelerated influx of nutrients promoted primary productivity, resulting in oxidation of dissolved organic carbon (DOC), whereas active sulfate reduction due to a higher sulfate influx from the continents caused remineralization of the large DOC, both of which caused a negative $\delta^{13}C$ anomaly. The 580 Ma Gaskiers glaciation accounts for the close correlation among the positive $^{87}Sr/^{86}Sr$, negative $\delta^{13}C$ and positive $\delta^{18}O$ excursions.

The second large positive shift of $^{87}Sr/^{86}Sr$ firstly accompanied a positive $\delta^{13}C$ excursion, and continued through the Shuram $\delta^{13}C$ negative excursion. The positive correlation of $\delta^{13}C$ and $^{87}Sr/^{86}Sr$ values is consistent with an enhanced continental weathering rate due to continental collisions that built Trans-Gondwana mountain chains, and with a higher primary activity due to the enhancement of continental weathering and consequent higher nutrient contents in seawater. The accompanied increase in Mn and Fe contents implies a gradual decline of the seawater oxygen content due to more active aerobic respiration and oxidation of reductive materials flowing in the oceans. In the Shuram excursion, higher $^{87}Sr/^{86}Sr$ values and a transition from increase to decrease in Mn and Fe contents were accompanied by the large negative $\delta^{13}C$ excursion. The higher $^{87}Sr/^{86}Sr$ values are the first compelling evidence for enhanced continental weathering, which was responsible for the large $\delta^{13}C$ anomaly through the remineralization of the DOC by more active sulfate reduction due to a higher sulfate influx. Higher Mn and Fe contents in the early and middle stages of the excursion suggest a decline in the oxygen content of seawater due to oxidative decay of the DOC, whereas in the late stages the decrease in Mn and Fe contents is consistent with oceanic oxygenation.

* Corresponding author. Tel.: +81 3 5734 2618; fax: +81 3 5734 3538.
E-mail address: sawaki.y.aa@m.titech.ac.jp (Y. Sawaki).

0301-9268/$ – see front matter
doi:10.1016/j.precamres.2009.10.006

The emergence of Ediacara biota after the Gaskiers glaciation and the prosperity of the latest Ediacaran is concomitant with the formation of more radiogenic seawater with high $^{87}Sr/^{86}Sr$ values, suggesting that enhanced continental weathering, and the consequent higher influx of nutrients, played an important role in biological evolution.

1. Introduction

The Ediacaran period records one of the most dramatic biological episodes in Earth history. Recent paleontological studies have clarified the emergence of two types of animals after the Marinoan glaciation in the Ediacaran of the Neoproterozoic (e.g. Sprigg, 1947; Glaessner and Wade, 1996; Brasier and Antcliffe, 2004; Xiao et al., 1998; Li et al., 1998; Chen et al., 2000). The Ediacaran fauna (Vendobionts) appeared in Australia, Siberia, Mackenzie Mountains, Western USA and Newfoundland, whereas cnidarians, sponges and possible bilaterians appeared in South China (Li et al., 1998; Chen et al., 2002, 2004; Xiao et al., 2000; Bengtson and Budd, 2004; Komiya et al., 2008a). Recent studies also demonstrate the existence of the Gaskiers glaciation at *ca.* 580 Ma (Bowring et al., 2003), after which most Ediacara fauna appeared (e.g. Narbonne and Gehling, 2003). However, the mode and origin of biological evolution are still ambiguous, because of the scarcity of well-preserved continuous successions of Ediacaran rocks. Many chemostratigraphies of Ediacaran age have been reported. However, their application to decoding the relationship between the surface environment and biological activity and evolution is restricted, because of lack of detailed multiple chemostratigraphy of C, O and Sr isotopes.

The weathering influx from continents is thought to be a major influence on the change in composition of ancient seawater and on biological evolution. Its flux can be estimated from the $^{87}Sr/^{86}Sr$ ratio of carbonate rocks. The $^{87}Sr/^{86}Sr$ composition of seawater mainly reflects a combination of non-radiogenic strontium derived from hydrothermal alteration of oceanic crust and radiogenic input from continental weathering. Due to the large isotopic difference between these two main sources of strontium, the $^{87}Sr/^{86}Sr$ composition of seawater tracks the long-term changes in the weathering of the continental surface relative to the hydrothermal flux (e.g. Richter et al., 1992). Shields and Veizer (2002) suggested that the radiogenic Sr isotope ratio suddenly increased in the Neoproterozoic based on the compilation of Sr isotope compositions through geologic time. Many previous studies of Sr isotope change from the Neoproterozoic to Cambrian vaguely showed that $^{87}Sr/^{86}Sr$ ratios had risen from *ca.* 0.707 around 635 Ma up to 0.7085 at the Precambrian/Cambrian boundary (Jacobsen and Kaufman, 1999; Shields, 1999; Melezhik et al., 2001; Kuznetsov et al., 2003; Halverson et al., 2007). However, $^{87}Sr/^{86}Sr$ measurements are still sporadic and insufficient for detailed discussion of surface environmental change and its influence on biological activity during the Ediacaran. No detailed and continuous $^{87}Sr/^{86}Sr$ data accompanied by detailed chemostratigraphies of $\delta^{13}C$ and $\delta^{18}O$ have been reported (Fig. 1).

South China is one of the best places to decode surface environments during the Ediacaran. We carried out on-land drilling of the Ediacaran Doushantuo Formation in South China, where there is a complete fossilferous sequence from the Neoproterozoic to the Cambrian, in order to make chemostratigraphies of $\delta^{13}C$, $\delta^{18}O$, and $^{87}Sr/^{86}Sr$ ratios. The drill-sampling enabled minimizing the effect of secondary alteration and oxidation on the surface so that we could make a very continuous chemostratigraphy at intervals of centimeters. This paper presents a new detailed chemostratigraphy of multi-isotopes of $\delta^{13}C$, $\delta^{18}O$, and $^{87}Sr/^{86}Sr$ in the Three Gorges region in South China, and their relevance to the change in composition of the ocean, with respect to changes in biological activity, surface environment and activity of the solid earth.

2. Geology of the Three Gorges Region

2.1. Geological setting

Neoproterozoic–Cambrian rocks crop out widely in South China; the Three Gorges is located *ca.* 30 km west of Yichang along the Yangtze River (Fig. 2a and b). The succession contains many fossils of Neoproterozoic and Cambrian age. In the Three Gorges region, shallow marine carbonates and deep-sea black shales were deposited in a palaeo-platform interior (Fig. 2a). Neoproterozoic and Phanerozoic successions surrounding the Huangling anticline are present in northwestern Yichang (Fig. 2b). The Neoproterozoic and Early Palaeozoic sections are especially well exposed along the Yangtze River cutting through the southern part of the anticline. Since the recognition of the Yangtze Gorges area as a type locality of the Sinian (Ediacaran) System (Lee and Chao, 1924; Liu and Sha, 1963), the Sinian sections of the area have been intensively investigated. The Three Gorges section consists of the Liantuo, Nantuo, Doushantuo, Dengying, Yanjiahe, Shuijintuo and Shipai Formations (Fm) in ascending order.

The succession of tillite, called the Nantuo Fm, rests directly on the Liantuo Fm with a sedimentary gap. The Nantuo Fm mainly consists of greenish tillite with a red sandstone layer in the middle. Tillite of the Nantuo Fm corresponds to glacial deposits of the Marinoan glaciation (Hoffman and Schrag, 2002).

The *ca.* 250 m thick Doushantuo Fm comprises the following four members in ascending order: Member 1 (Cap dolostone), Member 2 (black shale-dominated), Member 3 (dolostone-dominated) and Member 4 (black shale). The ~5 m-thick Member 1 is characterized by unusual sedimentary and diagenetic features such as stromatactis-like structures, tepee-like structures, sheet cracks, and barite fans in a cap carbonate (Jiang et al., 2003; Zhou et al., 2004). This member is divided into three subsequences in ascending order: a disrupted limestone/dolostone subunit, a laminated limestone/dolostone subunit, and a laminated silty limestone/dolostone subunit (Jiang et al., 2003). Member 2 contains many early diagenetic siliceous nodules with varied fossils of animal embryos, multicellular algae, acanthomorphic acritarchs, and filamentous and coccoidal cyanobacteria (Yin et al., 2007; Zhou et al., 2007; McFadden et al., 2008). The 6 m thick Member 4 is composed of black shale and is extremely enriched in organic carbon. Member 4 in the Miaohe section contains some species of Miaohe biota, e.g. *Enteromorphites siniansis*, *Sinospongia chenjunyuani* and *Sinospongia typica* (Xiao et al., 2002; McFadden et al., 2008). The age of the Doushantuo Fm in the Yangtze Gorges area is constrained by zircon U–Pb ages of three ash beds by the conventional TIMS method. The U–Pb zircon dates range from 635.2 ± 0.6 Ma for an ash bed within Member 1 through 632.5 ± 0.5 Ma for an ash at the bottom of Member 2, to 551.1 ± 0.7 Ma for an ash from the top of Member 4 (Condon et al., 2005). The ages of the last two ash beds were also determined by SHRIMP dates that are comparable with those of previous workers (Yin et al., 2005; Zhang et al., 2005). In summary, the Doushantuo Fm spans more than 80 million years, or roughly 90% of the Ediacaran Period.

The Dengying Fm in the Yangtze Gorges area corresponds to the top 10% of the Ediacaran Period. Its thickness varies from ~240 to 600 m (Zhao et al., 1988). It is composed of three Members: Hamajing, Shibantan and Baimatuo, in ascending order. The

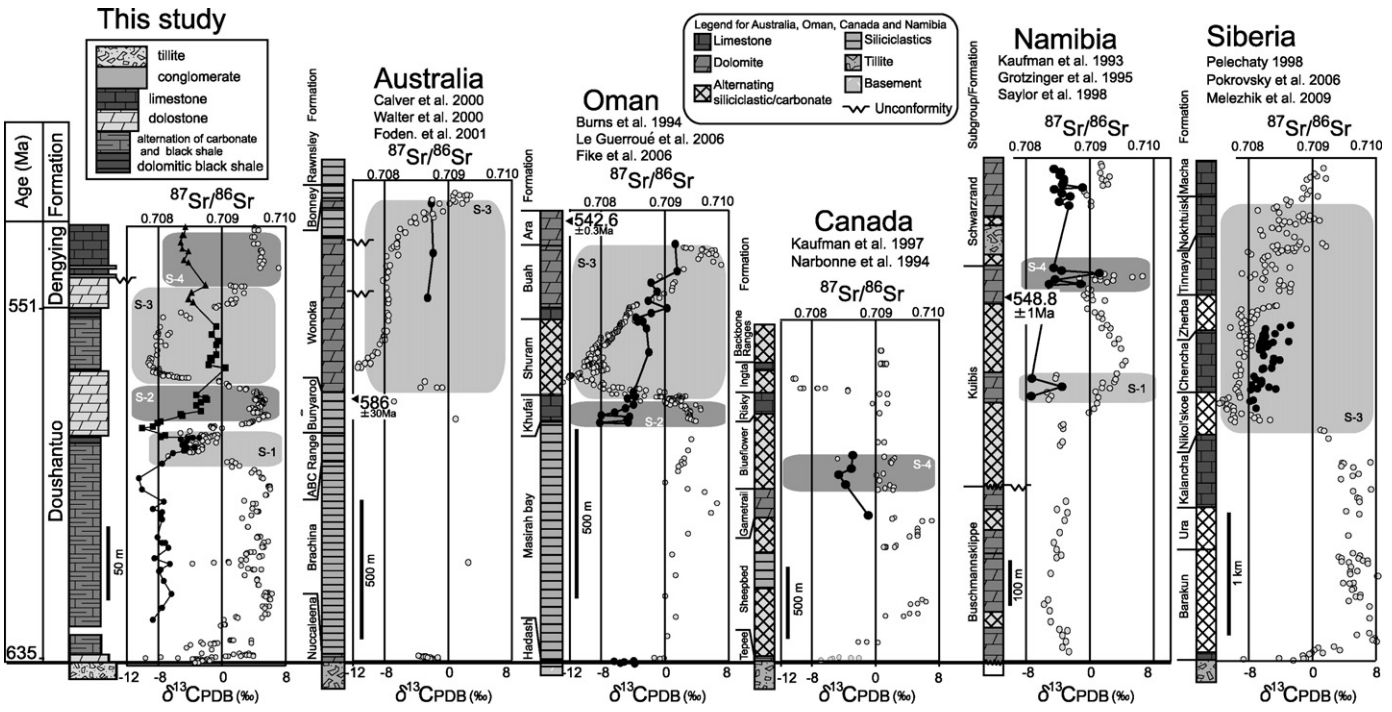

Fig. 1. Comparison of the Ediacaran chemostratigraphies of $\delta^{13}C$ and $^{87}Sr/^{86}Sr$ ratios in Australia, Oman, Canada, Namibia and Siberia (modified after Amthor et al., 2003; Calver, 2000; Walter et al., 2000; Foden et al., 2001; Burns et al., 1994; Le Guerroué et al., 2006; Kaufman et al., 1993, 1997; Narbonne et al., 1994; Grotzinger et al., 1995; Saylor et al., 1998; Pelechaty, 1998; Pokrovsky et al., 2006; Melezhik et al., 2009). Black points and black heavy lines mean excursions of $^{87}Sr/^{86}Sr$. Gray-filled circles show $\delta^{13}C$ ratios. Fields, shown as S-1–S-4, mark stratigraphic levels with similar isotopic values and patterns of $\delta^{13}C$ and $^{87}Sr/^{86}Sr$ ratios (see Section 5.1).

Hamajing Member, *ca.* 30 m thick, is characterized by massive intraclastic and oolitic dolomitic grainstone. The Shibantan Member, 100–160 m thick, has dark gray, thin-bedded limestones, and contains microbial structures, the algal fossil *Vendotaenia antiqua*, an Ediacaran macrofossil *Paracharnia dengyingensis*, possible Planolites-like trace fossils, and sponge spicules (Sun, 1986; Zhao et al., 1988; Steiner et al., 1993; Xiao et al., 2005). The Baimatuo Member consists of 40–400 m-thick, massive micritic and recrystallized dolomite, and in some areas an erosional surface was found at the top (Zhu et al., 2003). The tubular fossil, *Sinotubulites*, which may represent the earliest shell-producing metazoan, was reported in the lower part of the Baimatuo Member (Chen et al., 1981).

The Yanjiahe Fm is composed of an alternation of black limestone, and black dolostone, clastic sediments and black shale. The Yanjiahe Fm contains the key Small Shelly Fossils (SSFs), *Protohertzina anabarica* and *Anabarites trisulcatus* for Stage 1 and *Aldanella* for Stage 2 (proposed by Zhu et al. (2007) and Babcock and Peng (2007)). So, the Precambrian/Cambrian boundary is located within the Yanjiahe Formation. Some species of acritarchs (*Asteridium–Heliosphaeridium–Comasphaeridium* assemblage) are reported in the middle of the Yanjiahe Fm and the same assemblage is also reported from basal Cambrian strata in Tarim (Ding et al., 1992; Yao et al., 2005; Dong et al., 2009). The Shuijintuo and Shipai Formations mainly consist of black shale, clastic sediments and a few carbonates.

2.2. Stratigraphy of the Wuhe-Gaojiaxi section

The Ediacaran System in the Yangtze Gorges area was deposited on the Western Hubei platform. The Wuhe-Gaojiaxi section in the SE of Zigui near Yichang, Hubei Province (Fig. 2b and c), is one of the best known sections in the Yangtze Gorges region (e.g. Chen, 1987). The section is located on a north-facing cliff, which is exposed along the paved road from Zigui to Gaojiaxi in the south of Sandouping. Above the unconformity on the Huangling Granite, the section comprises the Liantuo, Nantuo (Marinoan-aged tillite), Doushantuo, Dengying, Yanjiahe, Shuijintuo and Shipai Fms in ascending order. Since 2005 we carried out drilling in this area from the Marinoan glaciation to the early Cambrian. Site 1 is about 268 m thick, and ranges from the bottom of Member 2 of the Doushantuo Fm through the Hamajing Member to the Shibantan Member of the Dengying Fm (Fig. 2d). Site 2 is about 130 m thick and ranges from the Liantuo Fm through the Nantuo Fm and to the bottom of Member 2 of the Doushantuo Fm (Fig. 2d); bedding planes dip to the SE by *ca.* 10–20°. The lithostratigraphy of drill-core samples is reconstructed in apparent thickness, because the difference between true and apparent thickness is less than 2–5% (Figs. 1, 3, 7 and 9). There may be missing between drill-core Sites 1 and 2 (Fig. 3).

Site 2 drill core contains the upper part of the Nantuo Fm, which is composed of tillite with pebbles to boulders (less than 10% in modal abundance) in a green, reddish, and dark-gray matrix. A Cap dolostone (*ca.* 6 m thick) with veins containing dark organic matter rests on the tillite. Above the Cap carbonate is a predominant black shale intercalated with lime-sandstone and dolostone (Fig. 3).

The Site 1 drill core comprises the Doushantuo Fm from Member 2 (*ca.* 120 m thick) of black shale with thin dolostone layers and tiny pyrite grains, through Member 3 (~80 m thick) of medium- to thick-bedded dolostones to Member 4 (~6 m thick) of black shale with thin limestone. Two flooding surfaces are identified in the Doushantuo Fm at the Member 2/3 boundary and Member 3/4 boundary in the Three Gorges area (Zhu et al., 2007). In addition, unconformities in the Wanjiagou and Xiaofenghe sections near the Three Gorge area are present around the boundaries of Member 2/3 and Member 3/4 (Zhu et al., 2007). The Dengying Fm rests conformably on the Doushantuo Fm. The Hamajing Member is composed of an upper wavy layer and lower stratified dolostones. A black to dark-gray bedded limestone of the Shibantan Member unconformably overlies the Hamajing dolostones, and is enriched in organic carbon (Fig. 4e).

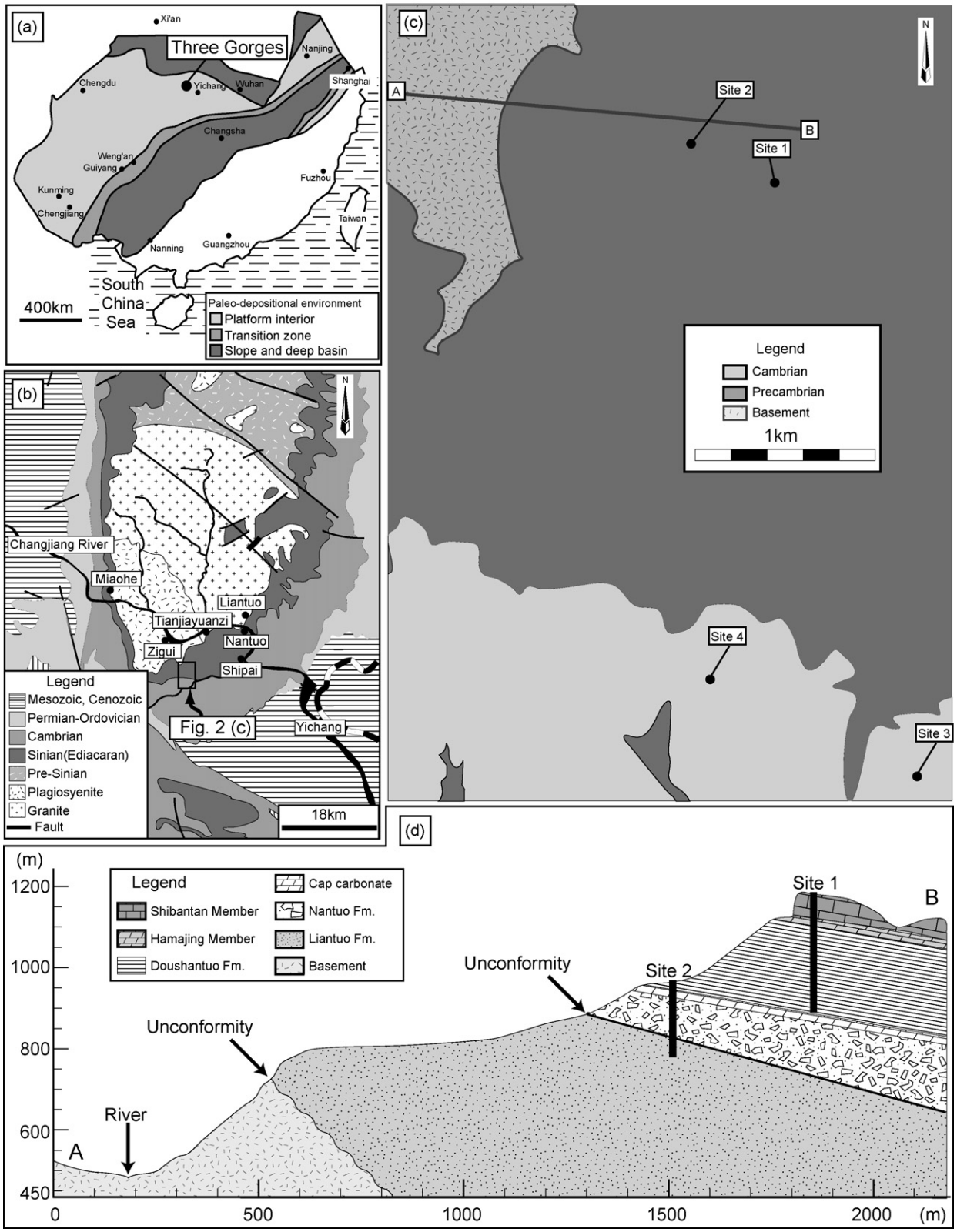

Fig. 2. (a) Simplified paleogeographic map of the Yangtze Platform around 600 Ma (modified after Zhu et al., 2003). Large circles indicate our study area. (b) Geological map of the Yangtze Gorges area, South China, showing our study area along the Yangtze River. (c) Simplified geological map of the Wuhe-Gaojiaxi region, Three Gorge area. Sites 1–4 represent our drilling positions. Sites 1 and 2 extend from the Liantuo Formation in the Cryogenian to the Shibantan Member of the Dengying Formation in the Ediacaran, whereas Sites 3 and 4 extend from the terminal Ediacaran to the early Cambrian (Ishikawa et al., 2008; Sawaki et al., 2008). (d) Schematic cross-section along line A–B in (c).

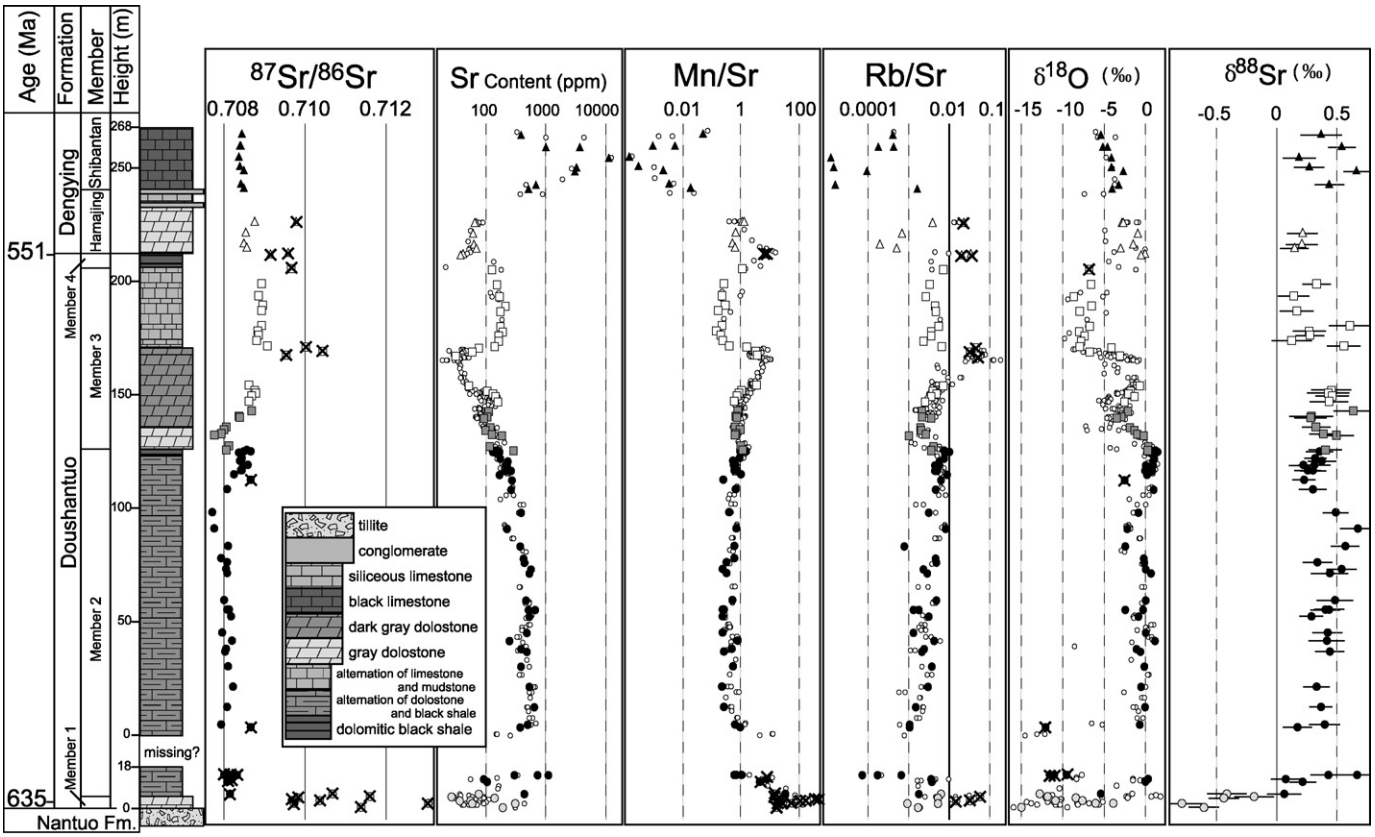

Fig. 3. Lithostratigraphic column and chemostratigraphies of $^{87}Sr/^{86}Sr$, Sr content, Mn/Sr, Rb/Sr, $\delta^{18}O$ and $\delta^{88}Sr$ of drill-core samples in the Three Gorges area, South China. Legends in chemostratigraphies of $^{87}Sr/^{86}Sr$ and $\delta^{18}O$ values are the same as those in Fig. 5. The $\delta^{18}O$ values are from Tahata et al. (submitted for publication). $^{87}Sr/^{86}Sr$ ratios were not analyzed for those samples marked as open circles in the Sr content, Mn/Sr, Rb/Sr, and $\delta^{18}O$ panels. Crosses on the marks mean altered samples, as the criteria are mentioned in Sections 4.1 and 4.2.

2.3. Petrography of the studied rock samples

We carefully conducted microscopic observations, and estimated the involvement of clastic and carbonaceous materials, and post-depositional oxidation, dissolution and alteration.

Pale gray dolostones of the Cap carbonate (Member 1) consist of anhedral dolomite with minor amounts of organic material (Fig. 4a). The size of dolomite crystals is irregular, up to 50 μm. We found thin, *ca.* 10 μm wide, dolomite veins and a few euhedral and anhedral pyrites. The rims of dolomite are still white and unoxidized. But some pyrites have a magnetite rim. Dark gray to gray dolostones of Member 2 and the lower part of Member 3 of the Doushantuo Fm contain fine-grained anhedral dolomites with minor amounts of clay minerals (micas) and detrital grains (e.g. plagioclase and quartz) less than 10 μm across. The distribution of organic material is homogeneous (Fig. 4b). A few pyrites are up to 10 μm across. All pyrites are still preserved even at their rims. Gray to pale gray dolostones of the upper part of Member 3 are mainly composed of abundant anhedral dolomites with minor clay minerals (micas) (Fig. 4c). The grain-size of the dolomite varies up to 80 μm. There are a few pyrites, most of which are euhedral, and the edges of some are altered to magnetite; a few iron hydroxides occur along grain boundaries. The distribution of organic material is homogeneous.

Dolostones in the Hamajing Member are gray to pale gray, and mainly consist of coarse-grained dolomite with minor clay and detrital minerals (Fig. 4d). The grain-size of the dolomite varies up to 70 μm. Dolomites are brownish in places due to the presence of iron hydroxide along grain boundaries in slightly altered samples. Black limestones of the Shibantan Member contain fine-grained anhedral calcites with minor amounts of clay minerals (micas) and detrital minerals. The grain-size of the detritus is less than 10 μm across. The distribution of organic material is homogeneous (Fig. 4e).

3. Sample preparation and analytical methods

We prepared rock powders from carbonate rocks and carbonate-dominant layers of alternating carbonates and black shales. In addition, rock powders were prepared by micro-drilling of small holes, millimeters across, on fresh surfaces of the drill-core samples of Sites 1 and 2 to avoid visible altered parts and veins of carbonate and quartz. However, extremely small amounts of tiny detritus may possibly be involved.

The powders were dissolved in 2 M acetic acid at 70 °C for 24 h in order to avoid dissolving the detrital silicate minerals. Ohno et al. (2008) also prepared rock powders from drill-core samples of Sites 1 and 2. The difference between Ohno et al. (2008) and this study is the acid: the former used hydrochloric acid, whereas we used weak acetic acid, the effect of which on dissolved silicate minerals will be discussed in Section 4.2. After insoluble residues had been removed from sample solutions, dissolved samples were evaporated and then re-dissolved in 2 M nitric acid. Any insoluble residue was excluded from the calculation of elemental concentrations.

We obtained Sr, Mn, Al, Si, Fe and K abundances with an inductively coupled plasma-optical emission spectrometer (ICP-OES, LEEMANS Labs. Ink., Prodigy) at the Center for Advanced Materials Analysis in the Tokyo Institute of Technology. Rb and Sr contents were also determined at the Tokyo Institute of Technology with an inductively coupled plasma-mass spectrometer (ICP-MS), which is a ThermoElemental VG PlasmaQuad 2 quadrupole-based ICP-MS equipped with an S-option interface (Hirata and Nesbitt, 1995). The

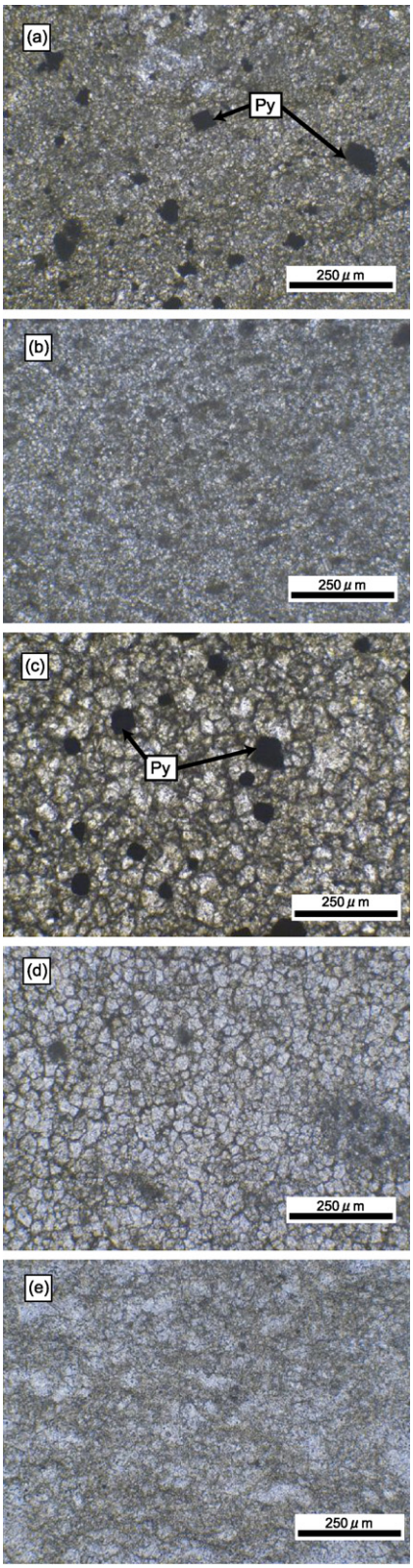

Fig. 4. Photographs of thin sections of (a) cap dolostone (fine-grained dolomite with anhedral and euhedral pyrites), (b) micritic to microspar gray dolostone in the lower part of Member 3, (c) coarse-grained pale gray dolostone in the upper part of Member 3, (d) coarse-grained pale dolostone in the Hamajing Member and (e) micritic black limestone in the Shibantan Member. Py: pyrite.

elemental abundances were obtained by calibration of peak intensities of sample solutions with an analytical standard solution, NIST 987 (Hirata et al., 1988).

In order to avoid the influence of an isobaric interference on ^{87}Sr, Sr was chemically separated from coexisting matrix elements (e.g. K, Mg, Ca, and Fe) and Rb using a chromatographic technique (Ohno and Hirata, 2006; Ohno et al., 2008). In this study, the samples dissolved in 2 M nitric acid were loaded onto *ca.* 0.25 ml of preconditioned Sr Spec column (i.d. 6 mm, height 10 mm, particle 50–100 μm). After matrix elements were removed by 5 ml of 7 M nitric acid and 3 ml of 2 M nitric acid, Sr were eluted by 5 ml of 0.05 M nitric acid.

Sr isotope compositions of ^{86}Sr, ^{87}Sr and ^{88}Sr were measured with a MC-ICP-MS (Nu plasma 500, Nu Instrument Ltd., Wrexham, Wales) at the Tokyo Institute of Technology. The operating conditions, including the torch position, Ar gas-flow rates and lens settings, were adjusted so as to maximize the signal intensity of ^{88}Sr (Ohno and Hirata, 2006; Ohno et al., 2008). Details of the instrument and the operating parameters are summarized in Table 1. An axial Faraday collector was used to measure 87 amu.

A correction of the mass discrimination effect is necessary for MC-ICP-MS measurements in order to obtain precise and accurate isotopic data. A typical mass discrimination effect of Sr observed in MC-ICP-MS measurements is 2–3% amu^{-1}. In this study, the mass discrimination effect was corrected by two correction techniques based on an exponential law (Russell et al., 1978). One is an internal correction technique, which provides the radiogenic ^{87}Sr/^{86}Sr isotope ratios using the non-radiogenic ^{86}Sr/^{88}Sr ratio of the international convention value determined by Nier (1938) as 0.1194 (Ohno and Hirata, 2006; Ohno et al., 2008). The other technique is an external correction using Zr, which corrects only the mass discrimination effect in a mass spectrometer (Ohno and Hirata, 2006; Ohno et al., 2008). Zr of NIST987 was added into both sample and analytical standard solutions. As a result, we obtained two isotopic ratios, ^{87}Sr/^{86}Sr and ^{88}Sr/^{86}Sr. The ^{88}Sr/^{86}Sr isotope ratios were expressed as the relative deviation from the ratio of an isotopic standard reference material (NIST NBS987) in terms of delta notations (δ).

$$\delta^{88}\mathrm{Sr} = \left[\frac{(^{88}\mathrm{Sr}/^{86}\mathrm{Sr})_{\mathrm{sample}}}{(^{88}\mathrm{Sr}/^{86}\mathrm{Sr})_{\mathrm{NIST}}} - 1\right] \times 1000$$

Table 1
Details of the instruments and the operation parameters.

(1) MC-ICP-MS instrument	
Nu instruments Nu Plasma	
(2) ICP Ion Source	
ICP	27.12 MHz
Power	1.35 kW forward, <5 W Ref.
Argon gas-flow rates	
Cooling	13 l/min
Auxiliary	0.7 l/min
Nebulizer	1.00–1.02 l/min
(3) Mass Spectrometer	
Ion energy	4000 V
Extraction	2400–2480 V
Analysis mode	Static
Ion detection	Analogue by Faraday
Typical transmission	80 V/(μg g^{-1})
Integration time	5 s
Scan-settled time	2 s
Number of cycles	40 cycles/run
Total analysis time	200 s/run
(4) Mass bias correction	
Internal correction	^{88}Sr/^{86}Sr
External correction	^{91}Zr/^{90}Zr

The detailed correction techniques are discussed in Ohno et al. (2008). The initial values of radiogenic $^{87}Sr/^{86}Sr$ isotope ratios were calculated from the minimum depositional ages, Rb/Sr ratios and a half-life of ^{87}Rb of 4.88×10^{10} years (Tables 2 and 3; see supplementary data files).

$\delta^{13}C$ and $\delta^{18}O$ data were compiled from the literature, but the analyses were carried out using the same rock powders with a Thermoquest GasBench II preparation device connected with helium flow to DELTA Plus XL at the Tokyo Institute of Technology (Tahata et al., submitted for publication).

4. Results

The chemical and isotopic compositions are summarized in Table 2 for Site 2 drill core, and Table 3 for Site 1 drill core. We estimated the influence of post-depositional alteration and detrital components to obtain primary $^{87}Sr/^{86}Sr$ values of the rock samples.

4.1. Post-depositional alteration

The isotopic compositions of Sr in marine carbonates are often susceptible to alteration. The processes of alteration may include early diagenetic transformations and late diagenetic fluid reactions. Alteration through interaction with clay minerals and groundwater, which have radiogenic isotopic compositions, would increase the $^{87}Sr/^{86}Sr$ ratios, whereas interaction with fluids from a juvenile volcanic source would decrease the $^{87}Sr/^{86}Sr$ values. Generally speaking, $^{87}Sr/^{86}Sr$ values increase due to post-depositional alteration (Brand and Veizer, 1980, 1981).

Previous workers cited ^{18}O-depletion, very low strontium content, very high manganese content, high Mn/Sr ratio, and conjugate decrease of $\delta^{13}C$ and $\delta^{18}O$ as characteristics of diagenetic alteration by meteoric water (Brand and Veizer, 1980, 1981; Banner and Hanson, 1990; Jacobsen and Kaufman, 1999; Halverson et al., 2007). In this study, we also checked correlations among the $^{87}Sr/^{86}Sr$ value, Sr and Mn contents, and $\delta^{13}C$ and $\delta^{18}O$ values.

All of the limestones in the Shibantan Member have high Sr and low Mn contents, and moderate $\delta^{18}O$ values (Fig. 5). The geochemical signature of moderate $\delta^{18}O$ values and no correlation among the $^{87}Sr/^{86}Sr$ ratio, Sr and Mn contents and $\delta^{18}O$ value, as well as our petrographic observations, suggest that the influence of secondary alteration through interaction with meteoritic fluids on the limestone samples is insignificant. Most samples of Member 2 and the lower part of Member 3 have high Sr and low Mn contents, moderate $\delta^{18}O$ values and no correlations between $^{87}Sr/^{86}Sr$ ratios, Sr and Mn contents and $\delta^{18}O$ values, suggesting that most samples preserve their primary $^{87}Sr/^{86}Sr$ values. However, a dolostone at the bottom of Member 2 has a very low $\delta^{18}O$ value, possibly affected by alteration. There is a slight negative correlation between $^{87}Sr/^{86}Sr$ and Sr contents in Member 1, the upper part of Member 3 of the Doushantuo Fm and the Hamajing Member of the Dengying Fm (Fig. 5). Post-depositional alteration shows such negative correlations (Brand and Veizer, 1980; Halverson et al., 2007), and some samples, which have very low Sr and very high Mn contents, might be affected by alteration.

The Mn/Sr ratio is also used for discrimination of diagenetic alterations, and the maximum Mn/Sr ratio of apparently unaltered samples ranges from 1 to 3 (Kaufman et al., 1993; Brasier et al., 1996; Kennedy et al., 1998; Jacobsen and Kaufman, 1999). The meteoric diagenesis model (Banner and Hanson, 1990; Jacobsen and Kaufman, 1999) shows that dolostone with very high Mn/Sr ratios from 10 to 40 might suffer isotopic modification of $\delta^{13}C$ and $\delta^{18}O$ ratios through interaction with meteoric fluids. In this study, most rock samples in Member 2 and the lower part of Member 3 of the Doushantuo Fm and in the Shibantan Member of the Dengying Fm have a low Mn/Sr ratio (<1). On the other hand, the Mn/Sr ratios in the lowermost of Member 2, upper part of Member 3 and the Hamajing Member range from 1 to 10 (Fig. 3). Cap carbonates in Member 1 have quite high Mn/Sr ratios (>10).

However, Mn contents and Mn/Sr ratios change according to the redox condition in the ocean, and $\delta^{18}O$ also changes according to the temperature in the ocean. Fig. 3 represents their stratigraphic changes to separate sub-trends by post-depositional alteration from general trends. Sr contents, Mn/Sr ratio and $\delta^{18}O$ of carbonates display smooth curves. Sr contents increase from *ca.* 50 ppm at the bottom of the Doushantuo Fm to *ca.* 500 ppm at the middle of Member 2 and gradually decrease down to *ca.* 40 ppm at around 170 m height. Above that height, Sr contents increase again in the upper part of the Member 3 and decrease again at the Doushantuo and Dengying Fms boundary. Limestones of the Shibantan Member have high Sr contents. Mn/Sr ratios provide a mirror image of the Sr contents. Mn/Sr ratios decrease from *ca.* 10 at the bottom of the Doushantuo Fm to *ca.* 0.5 in the middle of Member 2, and gradually increase up to *ca.* 5 at around 170 m. Afterwards, Mn/Sr ratios decrease again in the upper Member 3 and increase again at the boundary between the Doushantuo and Dengying Fms. Limestones of the Shibantan Member have low Mn/Sr ratios. $\delta^{18}O$ values in the cap carbonate and lower part of Member 2 vary between −15 and +1‰. $\delta^{18}O$ values fluctuate between −3 and +1‰ in the middle and upper part of Members 2. Two negative $\delta^{18}O$ anomalies, down to −7 and −10‰ respectively, are present in Member 3. $\delta^{18}O$ values in the Dengying Fm vary between −6 and 0‰. We removed $^{87}Sr/^{86}Sr$ data points with extremely high Mn/Sr ratios (>4) and/or low $\delta^{18}O$ values from the $^{87}Sr/^{86}Sr$ excursion curve compared with general trends (Fig. 3), because the samples are potentially affected by secondary alteration.

4.2. Influence of detrital components

Involvement of detrital materials influences Sr isotope compositions, because terrigenous detritus has radiogenic Sr isotopic compositions. Especially, the involvement of clay minerals and feldspar originating from continental crust significantly increases $^{87}Sr/^{86}Sr$ ratios, because they contain high Sr contents. Because clay minerals and feldspars contain higher Al, Si, K and Rb contents than carbonate minerals, we checked the correlations between $^{87}Sr/^{86}Sr$ ratios and Al, Si and K contents and Rb/Sr ratio to estimate the influence of a detrital component. The Rb/Sr ratio also reflects post-depositional alteration. In either case of post-depositional alteration or involvement of detritus, a high Rb/Sr ratio is unfavorable for the preservation of primary $^{87}Sr/^{86}Sr$ of carbonate rocks. Previous workers suggested a criterion of Rb/Sr < 0.001–0.01 for unaltered samples and detritus-free samples (Derry et al., 1989; Asmerom et al., 1991; Kaufman et al., 1993).

There is no correlation between $^{87}Sr/^{86}Sr$ ratios and Al, Si and K contents and Rb/Sr in Member 2, the lower part of Member 3, and the Shibantan Member, indicating an insignificant influence of clay minerals and feldspar on $^{87}Sr/^{86}Sr$ ratios (Fig. 6a–d). On the other hand, dolostone samples from Member 1 and the upper part of Member 3 have a faint correlation between $^{87}Sr/^{86}Sr$ ratios and Al, Si and K contents and Rb/Sr. Especially, four samples with higher $^{87}Sr/^{86}Sr$ ratio than 0.7095 have high Al, Si and K contents and Rb/Sr ratios. Dolostones of the Hamajing Member also have a positive correlation between $^{87}Sr/^{86}Sr$ ratios and Rb/Sr ratios. Petrographic observations show that the modal abundances of detrital materials are very low, but extremely high Rb/Sr ratios are unsuitable for reconstruction of the primary $^{87}Sr/^{86}Sr$ curve as mentioned above. So, we selected carbonate rocks with Rb/Sr < 0.01 as the unaltered and detritus-free samples (Fig. 6d). The influence of the detrital minerals is insignificant on the carbonate in Member 2, lower part of Member 3 and the Shibantan Member. No relation-

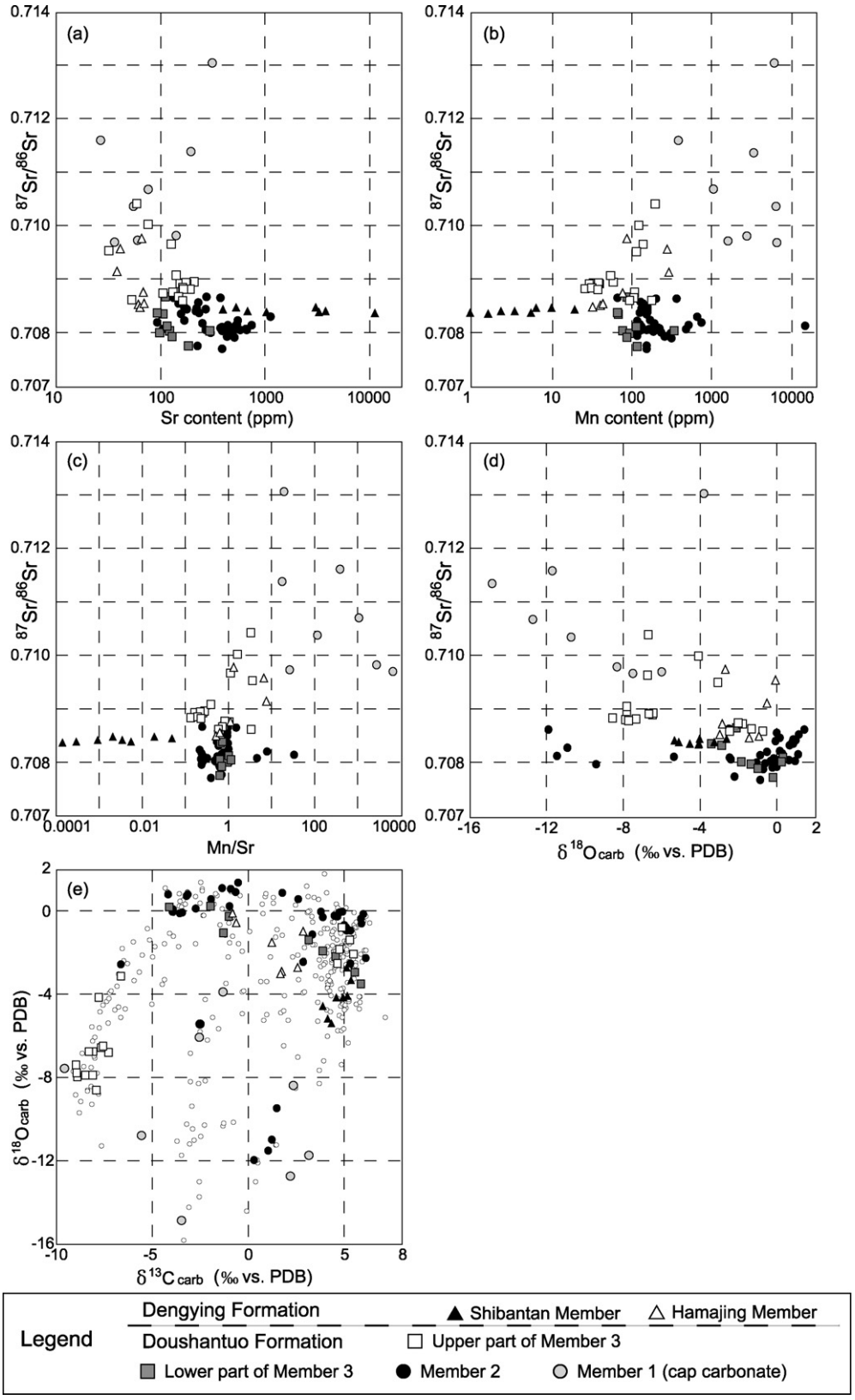

Fig. 5. Isotopic and elemental cross-plots of drill-core samples for $^{87}Sr/^{86}Sr$ vs. Sr contents, Mn contents, Mn/Sr and $\delta^{18}O$ (a–d). Isotopic cross-plot of $\delta^{18}O$ vs. $\delta^{13}C$ (e; data from Tahata et al., submitted for publication). The symbols are different for each stratigraphic Member. In Fig. 4, Member 3 is separated into lower and upper parts at the 145 m lithostratigraphic height.

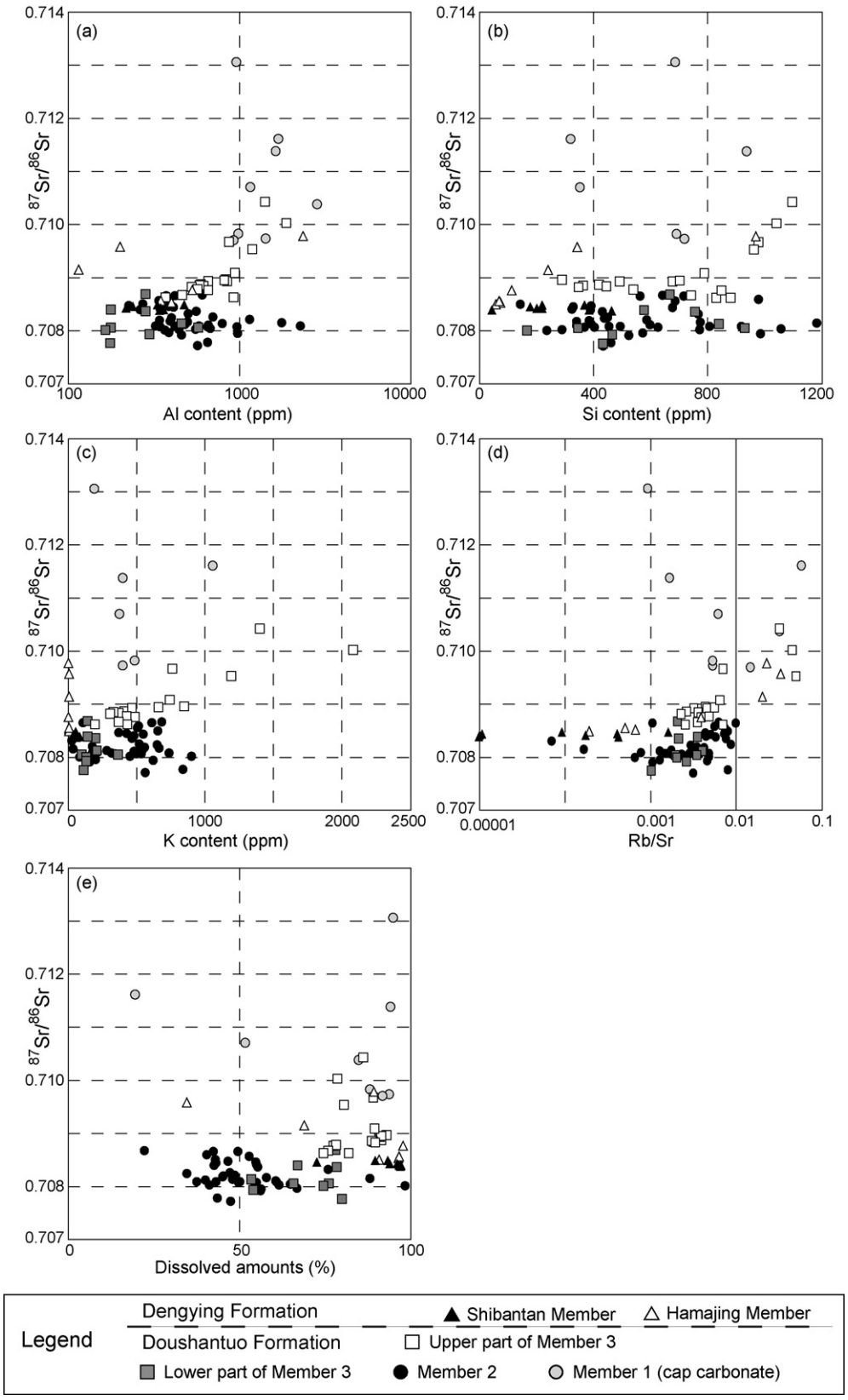

Fig. 6. Isotopic and elemental cross-plots of $^{87}Sr/^{86}Sr$ ratios and Al, Si and K contents and Rb/Sr ratios of drill-core samples (a–d). Cross-plots of $^{87}Sr/^{86}Sr$ ratios and ratios of dissolved amounts to insoluble residue (e). There is no clear correlation between $^{87}Sr/^{86}Sr$ ratios and these signatures, which indicate minor influence by involvement of detrital components. The symbols are the same as those in Fig. 4.

ship between $^{87}Sr/^{86}Sr$ and the ratio of the dissolved amount to insoluble residue also indicates that the influence of the detrital materials on the obtained $^{87}Sr/^{86}Sr$ isotope values is minor (Fig. 6e). Some dolostones in Member 1 and the Hamajing Member have a minor influence by involvement of detrital components, and were deleted (Fig. 6a–d).

4.3. Reconstruction of primary $^{87}Sr/^{86}Sr$ excursion in the Doushantuo and Dengying Formations

We obtained $^{87}Sr/^{86}Sr$ ratios of the least altered carbonate rocks from the Doushantuo and the Dengying Formations as mentioned above, and reconstructed the secular change of $^{87}Sr/^{86}Sr$ values of ancient seawater during the Ediacaran period (Fig. 7). The $^{87}Sr/^{86}Sr$ of carbonate rocks in the Doushantuo Fm gradually increased from *ca.* 0.708 to 0.709 with some positive and negative shifts. $^{87}Sr/^{86}Sr$ values of the lower part of Member 2 fluctuate around 0.708, and decrease to 0.7077 at *ca.* 100 m height. This is the lowest value in the Doushantuo Fm. The $^{87}Sr/^{86}Sr$ increases from 0.7077 to 0.7085 at *ca.* 120 m height of the top of Member 2. Subsequently, the $^{87}Sr/^{86}Sr$ value decreases to 0.7077 and increases again to *ca.* 0.709 through Member 3. The $^{87}Sr/^{86}Sr$ values of the limestone in the Shibantan Member are constant (*ca.* 0.7084). Previous workers showed a monotonous increase from 0.707 to 0.709 in $^{87}Sr/^{86}Sr$ ratio (Shields and Veizer, 2002; Halverson et al., 2007), but this work found two increases of $^{87}Sr/^{86}Sr$ ratio in the Ediacaran.

It is noteworthy that $^{87}Sr/^{86}Sr$, $\delta^{13}C$ and $\delta^{18}O$ values show good correlations (Fig. 7). The Sr isotopic compositions define a relatively smooth curve as a whole and two major positive shifts of $^{87}Sr/^{86}Sr$ are related to two major negative shifts of $\delta^{13}C$. We separated the Doushantuo and the Dengying Fms into four phases based on the $^{87}Sr/^{86}Sr$ ratio and $\delta^{13}C$. Phase-1 (P-1) comprises the lower part of the Doushantuo Fm and its upper boundary is defined by the beginning of increase in the $^{87}Sr/^{86}Sr$ ratio (Fig. 7). In the P-1, $^{87}Sr/^{86}Sr$ ratios fluctuate around 0.708. There is a faint negative correlation between $\delta^{13}C$ and $\delta^{18}O$ and a negative shift of $\delta^{13}C$ in the middle. A large positive excursion of $^{87}Sr/^{86}Sr$ ratio defines Phase-2 (P-2), that is by the minimum values on both sides of the excursion. In P-2, the $^{87}Sr/^{86}Sr$ ratio displays a sudden positive excursion, accompanied by $\delta^{13}C$ and $\delta^{18}O$ excursions. The timings of the decrease of the $\delta^{13}C$ and increase of the $\delta^{18}O$ are apparently identical. On the other hand, the changes in the $\delta^{13}C$ and $\delta^{18}O$ values slightly precede the increase of $^{87}Sr/^{86}Sr$ around the P-1/P-2 boundary. The $\delta^{13}C$ decreases from +5 to −4‰ and the $^{87}Sr/^{86}Sr$ ratio increases from 0.7077 to 0.7085. Subsequently, $\delta^{13}C$ increases up to −1‰ on the way up to *ca.* +5‰, and the $^{87}Sr/^{86}Sr$ ratio suddenly decreases to 0.7077. A large positive shift in the $^{87}Sr/^{86}Sr$ ratio and a positive $\delta^{13}C$ excursion define Phase-3 (P-3). The bottom boundary of P-3 is defined by the beginning of an increase in the $^{87}Sr/^{86}Sr$ ratio and the upper boundary of P-3 by the beginning of a decrease in $\delta^{13}C$ values. In P-3, the positive correlation between $^{87}Sr/^{86}Sr$ and $\delta^{18}O$ disappears. While $^{87}Sr/^{86}Sr$ increases from 0.7077 to 0.7087 and becomes constant, $\delta^{13}C$ increases to *ca.* +5‰ and $\delta^{18}O$ decreases to

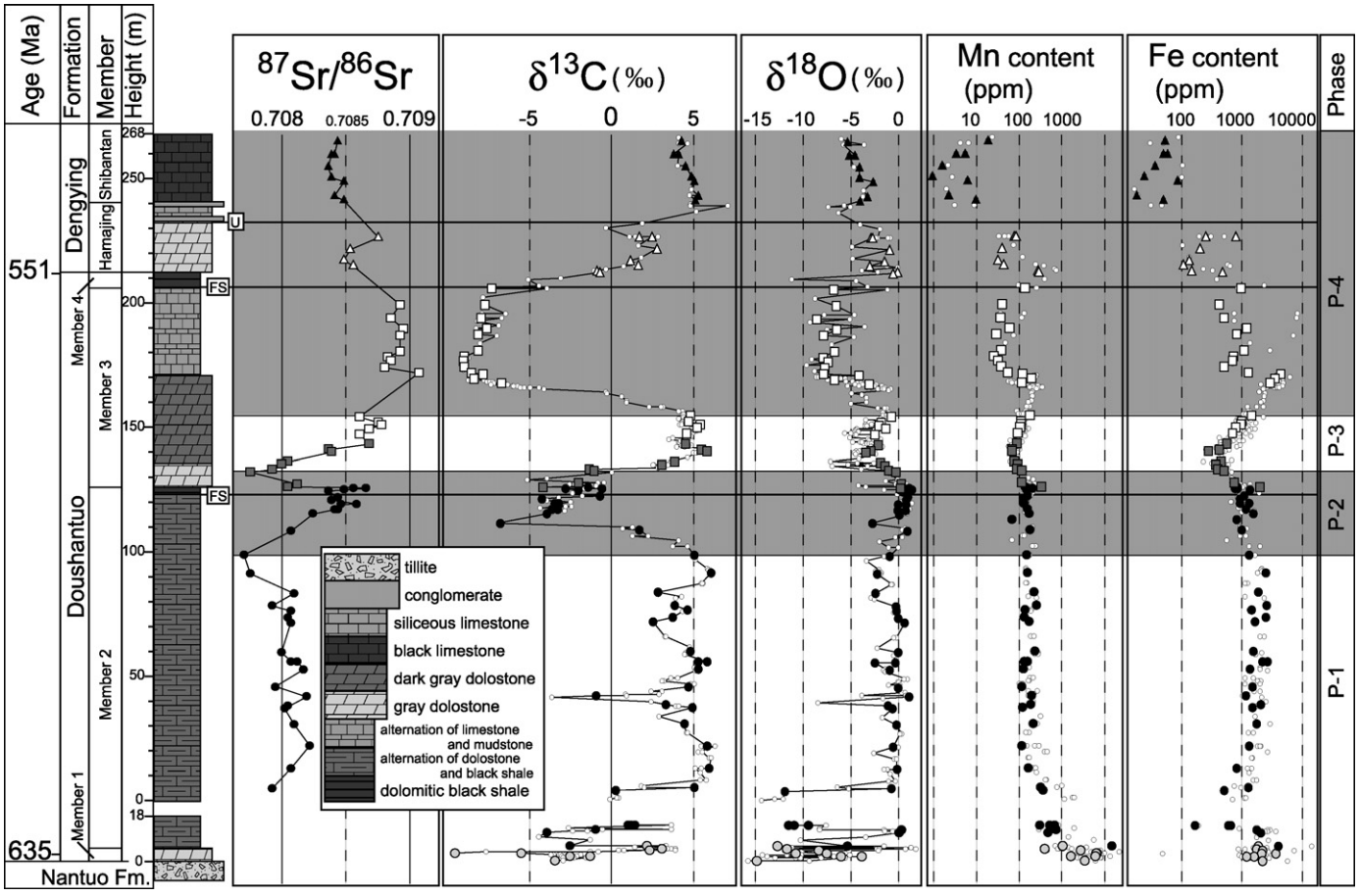

Fig. 7. Lithostratigraphic column and chemostratigraphies of $^{87}Sr/^{86}Sr$, $\delta^{13}C$, and $\delta^{18}O$ values, and Mn and Fe contents of drill-core samples in the Three Gorges area, South China. The $\delta^{13}C$ and $\delta^{18}O$ values are from the literature (Tahata et al., submitted for publication). Symbols in the $^{87}Sr/^{86}Sr$ chemostratigraphy are the same as those in Fig. 4. In the $\delta^{13}C$ and $\delta^{18}O$ chemostratigraphies, solid circles represent the same samples as $^{87}Sr/^{86}Sr$ analyses. Site 1 extends from 0 to 268 m in the upper part, whereas Site 2 extends from 0 to 18 m in the lower part. Capital "FS" means a flooding surface. Capital "U" means unconformity. Sr isotope excursion is separated into four phases based on the $\delta^{13}C$ and $^{87}Sr/^{86}Sr$ values. The definitions of Phases 1–4 are described in the text.

ca. −5‰. Phase-4 (P-4) ranges from the upper part of Member 3 to the Shibantan Member, and its bottom boundary is defined by the beginnings of a re-increase in $^{87}Sr/^{86}Sr$ and decrease in $\delta^{13}C$ values. In P-4, $\delta^{13}C$ and $\delta^{18}O$ decrease down to *ca.* −9‰ and −8‰, respectively, whereas $^{87}Sr/^{86}Sr$ values change from 0.7087 to the highest value of 0.7091. Subsequently, the $\delta^{13}C$ value gradually recovers to +5‰ and the $^{87}Sr/^{86}Sr$ ratios keep to medium values (*ca.* 0.7085) in the Dengying Formation.

We also obtained $\delta^{88}Sr$ from the Doushantuo and the Dengying Fms (Fig. 3). The $\delta^{88}Sr$ of carbonate rocks gradually increases from *ca.* −0.7‰ in the cap carbonate to *ca.* +0.1‰ at the bottom of Member 2. $\delta^{88}Sr$ values in the lower part of Member 2 fluctuate around +0.5‰, and slightly decrease to +0.3‰ at *ca.* 120 m height. $\delta^{88}Sr$ varies from +0.1‰ to +0.6‰ through Member 3. The $\delta^{88}Sr$ values of dolostone in the Hamajing Member are constant (*ca.* +0.2‰) but those of the limestone in the Shibantan Member relatively are variable between +0.2‰ to +0.6‰.

5. Discussion

5.1. Comparison with global excursions

At present the residence time of strontium in the oceans is from 2.5 to 4 million years (Elderfield, 1986; Hodell et al., 1990; Richter and Turekian, 1993), much longer than the surface and thermohaline ocean circulations, $\sim 10^3$ years (Broecker, 1982). Therefore, it is expected that the Sr isotopic composition is relatively homogeneous in the whole ocean. However, the exact residence time in the Ediacaran is not yet constrained. Hoffman et al. (1998) suggested that the Proterozoic ocean had higher Sr concentrations and a longer Sr residence time because of the lower Sr/Ca partitioning in inorganically precipitated carbonates.

$\delta^{88}Sr$ of carbonate rock is controlled by several parameters: (1) precipitation temperature of carbonate (Fietzke and Eisenhauer, 2006; Rüggeberg et al., 2008), (2) isotope variations of source materials (Ohno et al., 2008), and (3) the balance between efficiency of Sr sink and Sr content of seawater Sr, analogous to Ca isotopes (Lemarchand et al., 2004). The $\delta^{88}Sr$ values in the Ediacaran range from 0.3 to 0.6‰, except for some periods (Fig. 3). The lower Cap carbonate has quite low $\delta^{88}Sr$ values (Ohno et al., 2008), and the $\delta^{88}Sr$ values in P-2 and the upper Doushantuo Fm. are relatively low (Fig. 3). The quite low values in the Cap carbonate cannot be explained by its temperature dependence, because cap carbonate was formed during a relatively hot period (Hoffman et al., 1998). The isotopic variation of source materials from continental weathering may account for the low $\delta^{88}Sr$ values. However, the effect of isotopic variation of source materials is still ambiguous because all terrestrial rocks do not have a low $\delta^{88}Sr$. If Ediacaran seawater had a similar $\delta^{88}Sr$ value to modern seawater (*ca.* 0.35‰, Ohno et al., 2008; Halicz et al., 2008), the high $\delta^{88}Sr$ values in Members 2 and 3 of the Doushantuo and lower Dengying Formations indicate that Sr was more efficiently removed from seawater, and that the isotope fractionation of Sr was small, analogous to the Ca isotopes (Lemarchand et al., 2004; Komiya et al., 2008a). Namely, the high $\delta^{88}Sr$ values suggest that the Sr concentration of seawater was low relative to Sr removal so that the residence time of Sr was shorter in the Ediacaran. On the other hand, the low $\delta^{88}Sr$ values in some periods suggest relatively high Sr contents of seawater, and possibly higher continental influxes of Sr.

The $^{87}Sr/^{86}Sr$ compositions of carbonate rocks in the Three Gorges region are expected to reflect the global change of $^{87}Sr/^{86}Sr$, because the Yangtze platform was connected with an open ocean in those days (Zhu et al., 2003). Fig. 8 shows a comparison between this and previous studies in South China (Yang et al., 1999; W. Wang et al., 2002; Z. Wang et al., 2002; Jiang et al., 2007). Earlier studies analyzed Sr isotope compositions of carbonate rocks of outcrops in the Three Gorges. Our absolute values of the $^{87}Sr/^{86}Sr$ ratio in the middle of Member 2, the lower part of Member 3, and the Shibantan Member are consistent with previous studies, but the positive excursion of $^{87}Sr/^{86}Sr$ in P-2 and the increase of $^{87}Sr/^{86}Sr$ in P-3 were not identified previously. However, the scarcity of $^{87}Sr/^{86}Sr$ data in previous works suggests that the discrepancy results from the lack of Sr isotope data. Therefore, the $^{87}Sr/^{86}Sr$ chemostratigraphy of this work is consistent with that of previous studies, and it displays two new steep positive shifts and one steep negative shift in the Doushantuo Fm. W. Wang et al. (2002) reported very high $^{87}Sr/^{86}Sr$ values at the boundary between the Doushantuo and Dengying Fms. The high $^{87}Sr/^{86}Sr$ values are not recorded in our primary $^{87}Sr/^{86}Sr$ excursion. However, W. Wang et al. (2002) did not discuss post-depositional alteration. Our samples also record high $^{87}Sr/^{86}Sr$ values in the uppermost part of Member 3 and the lower part of the Hamajing Member, but their high Mn/Sr and Rb/Sr ratios indicate the effect of post-depositional alteration. Z. Wang et al. (2002) reported a very low $^{87}Sr/^{86}Sr$ value (0.7079) in the Hamajing Member. The rock sample has a high Rb/Sr ratio (*ca.* 0.028), unsuitable for preservation of primary $^{87}Sr/^{86}Sr$ of a carbonate rock.

Chemostratigraphies of both $\delta^{13}C$ and $^{87}Sr/^{86}Sr$ values during the Ediacaran period were reported in Australia, Oman, Canada, Namibia and Siberia (Kaufman et al., 1993, 1997; Burns et al., 1994; Saylor et al., 1998; Pelechaty, 1998; Calver, 2000; Walter et al., 2000; Le Guerroué et al., 2006; Pokrovsky et al., 2006; Melezhik et al., 2009, Fig. 1). There are many $\delta^{13}C$ studies in the Ediacaran, whereas a detailed $^{87}Sr/^{86}Sr$ study is still lacking. Recent $\delta^{13}C$ studies in the Chinese section clearly showed three major negative excursions at about 635 Ma in the lower Doushantuo, at 600–580 Ma in the middle of the Doushantuo, and at *ca.* 575–560 Ma in the upper Doushantuo Formation (Jiang et al., 2007; Zhou and Xiao, 2007; Zhu et al., 2007; McFadden et al., 2008). A negative $\delta^{13}C$ anomaly at about 635 Ma is ubiquitous in Cap carbonates in the world (Kaufman and Knoll, 1995; Hoffman et al., 1998). The last two $\delta^{13}C$ negative excursions are sporadically preserved in other sections in Australia, Oman, Namibia, northwestern Canada, western USA, Siberia and northern India. Previous workers correlated each other's data based on their $\delta^{13}C$ excursions (e.g. Halverson et al., 2005; Le Guerroué et al., 2006; Jiang et al., 2007; Zhou and Xiao, 2007; Zhu et al., 2007). For example, Le Guerroué et al. (2006) compared the upper Doushantuo excursion with the Wonoka in Australia, Shuram in Oman, Johnnie in Death Valley, USA, and Kuibis subgroup of the Nama Group, Namibia. On the other hand, Jiang et al. (2007) correlated it with a negative $\delta^{13}C$ anomaly in the Stirling Quartzite instead of the Johnnie Formation, USA, and correlated the middle Doushantuo excursions with that in the Johnnie Formation. We compare our results with those of previous studies by taking into account both $\delta^{13}C$ and $^{87}Sr/^{86}Sr$ changes, because the combination of $\delta^{13}C$ and $^{87}Sr/^{86}Sr$ chemostratigraphies clear shows that the middle and upper Doushantuo excursions have similar $\delta^{13}C$ negative values but different $^{87}Sr/^{86}Sr$ excursions.

The negative $\delta^{13}C$ values and low $^{87}Sr/^{86}Sr$ ratios (*ca.* 0.708) in the Namibian succession correspond to the negative excursion of $\delta^{13}C$ in Phase-2 of this study (Fig. 1; S-1). Similarly, the positive $\delta^{13}C$ and medium $^{87}Sr/^{86}Sr$ ratios (*ca.* 0.708–0.7085) in Oman are consistent with those in the lower part of Member 3 (Fig. 1; S-2). In the S-3, the $^{87}Sr/^{86}Sr$ ratios in the Three Gorges area change from *ca.* 0.7087 to 0.709 (Fig. 7). The $^{87}Sr/^{86}Sr$ ratios in Oman change from *ca.* 0.7086 to 0.7090, whereas three data points in the Australian section have 0.7087–0.7088 in $^{87}Sr/^{86}Sr$ ratios (Fig. 1). They are consistent with high $^{87}Sr/^{86}Sr$ values in the Chinese section during the Shuram excursion. However, there is a difference in $^{87}Sr/^{86}Sr$ variation in the Siberia section (Melezhik et al., 2009). The $^{87}Sr/^{86}Sr$ ratios in Siberia are relatively low, from 0.7080 at the early Shuram excursion, but they suddenly increase to 0.7086 in the middle.

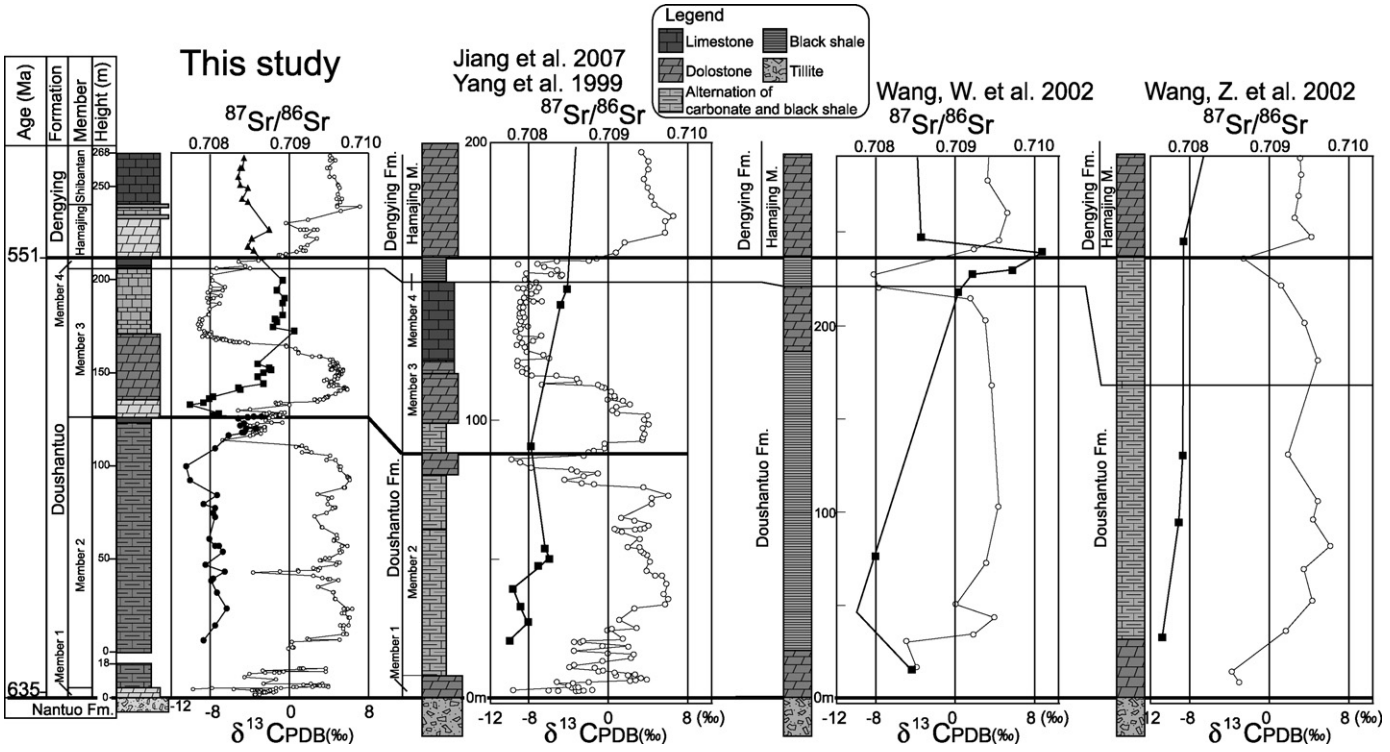

Fig. 8. Comparison of chemostratigraphies of $\delta^{13}C$ and $^{87}Sr/^{86}Sr$ ratios in South China (modified after Yang et al., 1999; W. Wang et al., 2002; Z. Wang et al., 2002; Jiang et al., 2007). Solid circles and black heavy lines mean excursions of $^{87}Sr/^{86}Sr$ values. Open circles and black narrow lines mean excursions of $\delta^{13}C$ values.

In general, the common characteristics are that Sr isotope values increased around the Shuram excursion, and the maximum value was over at least 0.7086, but the exact timing of the increase is still ambiguous and was probably variable among the oceans. Because there is a variation in $^{87}Sr/^{86}Sr$ ratios among present river waters (Palmer and Edmond, 1989; Richter et al., 1992), and because the residence time of Sr in seawater was shorter in the Ediacaran, $^{87}Sr/^{86}Sr$ values were possibly more varied especially in shallow marine environments than at present. However, the high $^{87}Sr/^{86}Sr$ (>0.7086) and low $\delta^{13}C$ values are common at the Shuram excursion in Oman, Australia and Siberia, which corresponds to S-3 in the Three Gorges area.

The positive $\delta^{13}C$ values and medium $^{87}Sr/^{86}Sr$ ratios (*ca.* 0.7085) in Namibia and Canada correspond to those in the Shibantan Member in our study (Fig. 1; S-4). Because no detailed $^{87}Sr/^{86}Sr$ isotopic compositions between the Marinoan glaciation and the first negative $\delta^{13}C$ excursion are available in other areas, it is still ambiguous to correlate the $^{87}Sr/^{86}Sr$ ratios in the middle and lower parts of Member 2 with successions in other areas. The $^{87}Sr/^{86}Sr$ curve of our work includes the majority of $^{87}Sr/^{86}Sr$ values of previous workers and potentially represents a global $^{87}Sr/^{86}Sr$ change in the Ediacaran. Our results demonstrate the first detailed $^{87}Sr/^{86}Sr$ excursion accompanied by a detailed $\delta^{13}C$ chemostratigraphy during the Ediacaran. In following section, we shall discuss the environmental changes that caused the two $^{87}Sr/^{86}Sr$ excursions (together with $\delta^{13}C$ and $\delta^{18}O$ changes) in the Ediacaran.

5.2. Where are the glacial deposits of the Gaskiers glaciation?

We have tried to constrain the position of the Gaskiers glaciation from the combined chemostratigraphies of $\delta^{13}C$, $\delta^{18}O$ and $^{87}Sr/^{86}Sr$. The chemostratigraphy of drill-core samples in the Three Gorges region indicates that positive $^{87}Sr/^{86}Sr$, negative $\delta^{13}C$ and positive $\delta^{18}O$ excursions are present around the Members 2–3 boundary (Fig. 7, P-2). The chemostratigraphies of the $\delta^{13}C$, $\delta^{18}O$ and $^{87}Sr/^{86}Sr$ ratios indicate the following features in P-2. Firstly, $\delta^{13}C$ decreases suddenly and $\delta^{18}O$ increases gradually from 91 m-height at almost the same time within the scattering of the data (Fig. 7). On the other hand, $^{87}Sr/^{86}Sr$ values increase gradually from 0.7077 at 99 m-height to 0.7085 at 116 m-height. Between *ca.* 116 and 126 m-height, $\delta^{13}C$, $\delta^{18}O$ and $^{87}Sr/^{86}Sr$ values fluctuate around −4‰, 0‰ and 0.7085, respectively. Later, $\delta^{18}O$ and $^{87}Sr/^{86}Sr$ simultaneously decrease, whereas $\delta^{13}C$ increase gradually at the bottom of Member 3.

Generally speaking, post-depositional alteration causes $\delta^{18}O$ to decrease, because the $\delta^{13}C$ of pore fluids is lower than that of seawater, and because the diagenetic reaction proceeds at a higher temperature than the precipitation of carbonate minerals under the sea. The increase of $\delta^{18}O$ values and negative correlation between $\delta^{18}O$ and $\delta^{13}C$ variations in the P-2 suggest that our drill-core samples still preserve the primary signatures of $\delta^{18}O$. In this case, the gradual increase in $\delta^{18}O$ indicates global cooling (Tahata et al., submitted for publication). Many unconformities, correlated with the negative $\delta^{13}C$ excursion, are found throughout the world: at Xiaofenghe and Wangjiagou in the Yangtze region (Zhu et al., 2007), the Death Valley area (Kaufman et al., 2007), and northern India (Jiang et al., 2002; Kaufman et al., 2006), suggesting a regression in the middle Ediacaran. A regression enhances continental weathering because a continental shelf is widely exposed, consistent with a high $^{87}Sr/^{86}Sr$ value. In addition, Phanerozoic $^{87}Sr/^{86}Sr$ studies also suggest a correlation between $^{87}Sr/^{86}Sr$ and a glacial period (Blum et al., 1993). Blum and Erel (1995) suggested that the $^{87}Sr/^{86}Sr$ ratio of Sr released at an early stage of weathering is significantly higher than that at a later stage, and that the $^{87}Sr/^{86}Sr$ ratio of a global riverine influx drastically increases at the early stage of glacial-cycling. Li et al. (2007) suggested that global cooling produced an increase in marine $^{87}Sr/^{86}Sr$ ratio since 3.4 Ma, and they emphasize the importance of low activation energy of mica minerals. The isotopic change is consistent with the positive shift of $^{87}Sr/^{86}Sr$ during the glaciation.

In a Phanerozoic analogue, it is expected that a glacioeustatic sea-level fall would cause a rise in seawater $\delta^{13}C$, because organic burial would be enhanced. The Late Ordovician glaciation, for example, is associated with a positive excursion in $\delta^{13}C$ (Kump et al., 1999). However, previous studies suggested that the carbon system in the Ediacaran differed from that during the Phanerozoic in terms of the size of dissolved inorganic carbon (DIC) and organic carbon (DOC) reservoirs, and of the efficiency of organic burials. The DOC reservoir was larger than the DIC reservoir in the Ediacaran (Rothman et al., 2003; McFadden et al., 2008), and the organic burial was less efficient (Rothman et al., 2003). Under such a carbon system, oxygen generated from accelerated primary productivity due to the higher nutrient content would be consumed by oxidation of the large DOC reservoir, and a higher sulfate influx from continents would promote remineralization of the DOC (Fike et al., 2006; Jiang et al., 2007), which in turn would decrease $\delta^{13}C$ in the ocean. In addition, Peltier et al. (2007) proposed a linkage between glaciation and a negative $\delta^{13}C$ excursion and emphasized the temperature-dependence solubility of oxygen. In their model, a high oxygen solubility during a glaciation leads to promotion of remineralization of the DOC. Global cooling apparently accounts for the geochemical correlations among the three isotope systems as well as geological evidence for global unconformities in the middle Ediacaran.

In summary, the chemostratigraphies of the $\delta^{13}C$, $\delta^{18}O$ and $^{87}Sr/^{86}Sr$ ratios in P-2 are explained by global cooling. Global temperature decreased, evident in the positive shift of $\delta^{18}O$. The enhanced primary activity due to high influx of nutrients promoted oxidation of the large DOC reservoir, and active sulfate reduction due to higher sulfate influx from continents enhanced remineralization of the DOC reservoir, both which are recorded as a negative shift of $\delta^{13}C$. The positive shift of the $^{87}Sr/^{86}Sr$ ratio indicates that the formation of glaciers on continents caused global regression and enhanced continental weathering, because of an increase in the erosional surface of continental crust. After the glaciation, the global temperature recovered, and $\delta^{13}C$, $\delta^{18}O$ and $^{87}Sr/^{86}Sr$ contemporaneously began to recover to the pre-glaciation values.

It is difficult to constrain the Gaskiers glaciation in the Three Gorges region, because no glacial deposit, corresponding to the Gaskiers glaciation, is found in South China. However, Condon et al. (2005) compiled chemostratigraphies in South China, and suggested the correlation of a faint negative value around the 2–3 Member boundary with negative $\delta^{13}C$ values of carbonate rocks above the Gaskiers Glaciation in Newfoundland (Myrow and Kaufman, 1999). Zhu et al. (2007) suggested a potential cause of the Gaskiers Glaciation for the negative excursion in the middle Doushantuo Formation based on compilation of $\delta^{13}C$ data in South China. On the other hand, some previous workers related the Shuram-Wonoka-upper Doushantuo excursion to the Gaskiers Glaciation (Le Guerroué et al., 2006; Halverson et al., 2005; Halverson, 2006).

Previous works showed $\delta^{13}C$ chemostratigraphies of the Weng'an sections, which have negative $\delta^{13}C$ values at the bottom, middle and top of the Doushantuo Formation (Zhou, 1997; Zhou et al., 2007; Zhu et al., 2007), and suggested that the negative $\delta^{13}C$ excursion around the boundary between Members 2 and 3 in the Three Gorges area is equivalent to the negative $\delta^{13}C$ excursion in carbonate layers at the top of the lower Doushantuo Formation (EN2; nomenclature in Zhou and Xiao, 2007) in the Weng'an area, and that the $\delta^{13}C$ negative excursion in P-4 of the Three Gorges area corresponds to the $\delta^{13}C$ negative excursion in the upper Doushantuo Fm (EN3) in the Weng'an area based on a comparison between the Three Gorges and Weng'an areas in terms of their $\delta^{13}C$ chemostratigraphy and sequence stratigraphy (e.g. Zhou and Xiao, 2007; Zhou et al., 2007; Zhu et al., 2007). In this case, the $\delta^{13}C$ negative excursion of P-2 is possibly placed before the 580 Ma Gaskiers Glaciation (Zhou and Xiao, 2007; Zhou et al., 2007), because a Pb–Pb age of phosphorite above the excursion is 599 ± 4 Ma (Barfod et al., 2002).

However, recent studies showed more complicated $\delta^{13}C$ variations in the Weng'an section: the $\delta^{13}C$ negative excursion at the middle Doushantuo Fm is split into two (Zhou and Xiao, 2007) or three parts (Zhu et al., 2007), and there is large and frequent fluctuation between −4 and +1‰ in the upper Doushantuo Fm (Zhou et al., 2007). In addition, two negative $\delta^{13}C$ excursions are found between the EN2 and EN3 (Zhu et al., 2007). Moreover, new chemostratigraphic and stratigraphic studies reported much more complicated $\delta^{13}C$ chemostratigraphy, and more local exposures of dolograinstone layers in the middle to upper Doushantuo Formation (Jiang et al., 2008). The occurrence of more widespread local exposures is consistent with a very shallow water environment (Vernhet, 2007; Jiang et al., 2008), possibly susceptible to local sea-level change. The difference in the patterns and absolute values of the $\delta^{13}C$ chemostratigraphies supports the idea that the Weng'an section represents a shallow water environment and does not possess all the global signatures. In addition, the geochronological data of Barfod et al. (2002) has some ambiguities to evaluate the accuracy of the calculated dates: the complexity of diagenesis in phosphorites and the use of leached whole-rock samples that span several meters of section (Condon et al., 2005). Recently, multicellular algae, animal embryo fossils and acritarchs fossils, equivalent to those at the Upper phosphorite unit in the Weng'an area (e.g. Xiao et al., 1998), were found in the lowest part of Member 2 in the Three Gorge area (Xiao et al., 1998; Zhou et al., 2007; Yin et al., 2007; McFadden et al., 2008; Liu et al., 2009). If the biostratigraphies are mutually correlated, the Upper Member of the Doushantuo in Weng'an corresponds to the lower Member 2 in the Three Gorges area.

There is no compelling evidence for a single glaciation during the Ediacaran, but the Gaskiers glaciation is widely accepted as one of the Ediacaran glaciations. In addition, the $\delta^{18}O$ values in Member 2 are relatively high, but the largest $\delta^{18}O$ positive excursion is found in the P-2 (Tahata et al., submitted for publication). The most distinctive change in the combination of $\delta^{18}O$, $\delta^{13}C$ and $^{87}Sr/^{86}Sr$ values is also present in P-2. Although a more severe glaciation than that of the Gaskiers glaciation can be assumed in the middle Ediacaran, the present lines of evidence suggest that the glaciation in P-2 is the Gaskiers glaciation.

5.3. Enhanced continental weathering and the Shuram negative carbon isotope excursion

A large negative isotope excursion is found in the middle Ediacaran from *ca.* 575 to 550 Ma, the so-called the Shuram excursion, in Oman, Australia, Namibia, western United States, northern India, Svalbard, Siberia and South China (Condon et al., 2005; Halverson et al., 2005; Saylor et al., 1998; Le Guerroué et al., 2006; Fike et al., 2006; Pokrovsky et al., 2006; Kaufman et al., 2007; Jiang et al., 2007; McFadden et al., 2008; Melezhik et al., 2009). The cause of the Shuram excursion is still controversial. Fike et al. (2006) showed no correlation between $\delta^{13}C_{carb}$ and $\delta^{13}C_{org}$ through the Shuram excursion, and provided evidence to support the idea of Rothman et al. (2003) for the existence of a large DOC reservoir. Fike et al. (2006) also demonstrated a high $\Delta\delta^{34}S$ through the excursion, and suggested that an increase in the content of oceanic sulfate derived from continental weathering due to high atmospheric O_2 enhanced sulfate reduction and caused remineralization of the DOC. In addition, the beginnings of a positive correlation between $\delta^{13}C_{carb}$ and $\delta^{13}C_{org}$ at a late stage of the excursion suggest the disappearance of the excess DOC reservoir, namely a fully oxidized state (Fike et al., 2006).

However, Kaufman et al. (2007) analyzed sulfur isotope ratios of Ediacaran rocks in Death Valley, USA and pointed out that the sulfur

isotope excursion was not sufficient to cause the large negative $\delta^{13}C$ anomaly; as an alternative they proposed oxidation of fossil organic material trapped in marginal marine sediments and exposed sediments. The strong negative $\delta^{13}C$ anomaly results from river input of oxidized organic material (Kaufman et al., 2007), which is apparently consistent with high $^{87}Sr/^{86}Sr$ during the Shuram excursion. However, oxygen deficiency of seawater in the early stage, as described in detail below, prefers remineralization of the DOC rather than input of oxidized organic materials. Recently, assuming that the rate of decay of the excess DOC pool was initially set as a linear function of DOC concentration, Bristow and Kennedy (2008) calculated the size of the DOC reservoir and inspected the duration of the negative $\delta^{13}C_{carb}$ anomaly with a nadir of the negative $\delta^{13}C$ anomaly at −12‰. The calculation shows a very short duration of the $\delta^{13}C_{carb}$ change and a quick exhaustion of oxygen and sulfate in seawater. Bristow and Kennedy (2008) suggested that the large negative $\delta^{13}C$ excursion occurred in salinity-stratified basins with limited marine connections. However, the ubiquitous occurrence of the Shuram excursion in Oman, Australia, South China, western United States, Svalbard, Siberia and northern India is inconsistent with a local event in a closed basin. Moreover, it is possible that a much larger DOC reservoir and a slower remineralization of the DOC caused a longer duration of the $\delta^{13}C$ excursion, because the validity of the assumption of a linear relationship between the decay rate and the DOC concentration is still ambiguous.

As a result, a remineralization of the DOC due to an enhancement of the sulfate influx and oxidative weathering of organic carbon in exhumed sediments still accounts for the large negative $\delta^{13}C_{carb}$ better than any other models. However, previous workers showed no compelling evidence for the enhancement of continental weathering during the Shuram excursion. Our chemostratigraphy clearly demonstrates a sudden increase in $^{87}Sr/^{86}Sr$ ratio through the Shuram excursion consistent with a rise in continental weathering and with the hypothesis that a high continental influx of sulfate caused the large negative $\delta^{13}C_{carb}$ excursion (Fike et al., 2006; McFadden et al., 2008).

Sulfate is supplied to the ocean by dissolution of sulfate-bearing minerals and oxidative weathering of pyrite exposed on land. Earlier workers assumed an increase of oxidative weathering of sulfide in the Shuram excursion (Fike et al., 2006; Jiang et al., 2007; McFadden et al., 2008). However, it is still controversial whether the oxygen content of the atmosphere and seawater increased around the Shuram excursion (e.g. Bristow and Kennedy, 2008). The ratio of highly reactive iron such as iron oxide, carbonate and sulfide minerals, to total iron (Fe_{HR}/Fe_T) indicates an increase in the oxygen content of seawater after the Gaskiers glaciation (Canfield et al., 2007, 2008). Although there are only few data, the Ce anomaly of carbonate rocks suggests that shallow seawater became anoxic after the Gaskiers Glaciation (Yang et al., 1999; Komiya et al., 2008b). The gradual increase of sulfur isotope fractionation between sulfate and sulfide, $\Delta\delta^{34}S$ (Hurtgen et al., 2005; Fike et al., 2006), was interpreted as an increase of atmospheric oxygen through the Ediacaran (Fike et al., 2006). The evidence suggests that the oxygen content of seawater did not increase just before the Shuram excursion and at an early stage.

The major sources of marine manganese and iron are a hydrothermal influx from oceanic crust and river input from continental weathering. Major sinks of these elements are authigenic minerals (oxide and carbonate), absorption and biological intake. The Mn and Fe contents, generally speaking, are mainly controlled by the redox condition of the ocean. Mn and Fe are easily oxidized and precipitated as oxide and oxyhydroxide minerals under an oxic condition, whereas Mn^{2+} and Fe^{2+} are stable and accumulate in an anoxic condition. The Mn^{2+} and Fe^{2+} are involved in a solid solution in carbonate minerals. Assuming that the partition coefficients of Mn and Fe between seawater and carbonate minerals are constant, the Mn and Fe contents of carbonate minerals reflect a redox condition; higher Mn and Fe contents under an anoxic condition. Mn and Fe contents of carbonate rocks decreased just after the Gaskiers glaciation and then increased, supporting a sudden increase of the oxygen content after the glaciation based on the Fe_{HR}/Fe_T ratio (Canfield et al., 2007) and the following decline of oxygen content based on the Ce anomaly of carbonate (Yang et al., 1999; Komiya et al., 2008b) (Fig. 7). In the final stages, Mn and Fe contents decreased, consistent with an increase of oxygen content shown by the beginning of coupling between $\delta^{13}C_{carb}$ and $\delta^{13}C_{org}$ and a high $\Delta\delta^{34}S$ value (Fike et al., 2006). The above line of evidence suggests that the rise in atmospheric oxygen was not a trigger for the enhancement of the oceanic sulfate influx and the consequent Shuram $\delta^{13}C$ negative excursion.

5.4. A surface environmental change induced by continental collision

We will now discuss surface environmental changes in P-3 and P-4 based on the detailed chemostratigraphy of our drill-core samples in the Three Gorges region (Fig. 7). The $^{87}Sr/^{86}Sr$ ratio suddenly increased in P-3, and $\delta^{13}C$ increased up to +5‰, and $\delta^{18}O$ decreased. During P-4, $\delta^{13}C$ and $\delta^{18}O$ decreased to their lowest values, and $^{87}Sr/^{86}Sr$ reached *ca.* 0.7092, comparable to the $^{87}Sr/^{86}Sr$ ratio of present seawater. There was a large positive $^{87}Sr/^{86}Sr$ shift accompanied by a positive $\delta^{13}C$ shift, and these clearly preceded the large negative shifts of $\delta^{13}C$ and $\delta^{18}O$, namely the Shuram excursion. The positive correlation of $\delta^{13}C$ and $^{87}Sr/^{86}Sr$ changes is apparently different from the negative correlation between $\delta^{13}C$ and $^{87}Sr/^{86}Sr$ values at the 580 Ma Gaskiers glaciation, as mentioned above. Generally speaking, the following processes account for the increase in the $^{87}Sr/^{86}Sr$ ratio of seawater: sea-level fall, formation of mountain chains due to continental collision (Richter et al., 1992), a decrease in the input of mantle Sr due to inactive hydrothermal activity and volcanism (Shields, 2007), and enhancement of continental weathering due to global warming. A regression event due to an extensive glaciation is inconsistent with the low $\delta^{18}O$ values. Shields (2007) suggested that a reversible increase in the overall continental weathering rates due to tectonic uplift is the most plausible explanation based on the normalized $^{87}Sr/^{86}Sr$ curve, a published seawater $\delta^{34}S$ curve and atmospheric pCO_2. As a modern analogue, it is well known that the uplift of the Himalaya and Tibetan Plateau increased continental weathering rates, and resulted in a more radiogenic Sr isotope ratio of seawater (Richter et al., 1992). Squire et al. (2006) suggested the convergence of East and West Gondwana at 650–500 Ma and the consequent formation of a Transgondwanan Supermountain between the two supercontinents to trigger the biotic and isotopic explosions. The most extensive development of uplifted mountains started at 590 Ma, when the East African margin collided with India and Madagascar (Boger and Miller, 2004; Squire et al., 2006). Continental convergence can explain the sudden increase of $^{87}Sr/^{86}Sr$, suggesting that the formation of a mountain chain between East Africa, India and Madagascar (590–550 Ma) possibly caused the higher continental weathering in P-3. The difference between onset of continental collision (590 Ma) and beginning of $^{87}Sr/^{86}Sr$ excursion (after 580 Ma) is explained by the fact that $^{87}Sr/^{86}Sr$ began to change *ca.* 10 million years later than the collision (Himalaya and Tibetan Plateau) in the Cenozoic (Richter et al., 1992). The higher continental weathering resulted in enhanced primary productivity due to the consequent high nutrient influx, which is preserved as a positive shift of $\delta^{13}C$.

A large negative $\delta^{13}C$ anomaly in P-4 corresponds to the Shuram excursion and records a nadir of −12‰, and the $\delta^{18}O$ value also reaches *ca.* −8‰, as mentioned above. Because negative $\delta^{13}C$ values below −6‰ (mantle value) cannot be explained by a suppression

of primary productivity and enhanced volcanism, an injection of pools of depleted carbon is required such as the dissolution of methane hydrates (Dickens et al., 1995), an oxidative decay of exposed marine organic sediments (Higgins and Schrag, 2006), and ocean stagnation and overturn (Knoll et al., 1996; Yang et al., 1999). Previous workers suggested oxidation of the DOC as the source (Fike et al., 2006; Jiang et al., 2007; McFadden et al., 2008).

The decrease of Mn and Fe contents, accompanied by a $\delta^{13}C$ positive shift, from the late stage of P-2 to early P-3 suggests oxidation possibly due to the high primary productivity (Fig. 7), and this supports oxidation based on a decrease in the Fe_{HR}/Fe_T ratio after the Gaskiers glaciation (Canfield et al., 2007). The onset of the increase in Mn and Fe contents is concomitant with the beginning of a plateau of $\delta^{13}C$. The increase in Mn and Fe contents continued until the minimum values were reached of $\delta^{13}C$ and $\delta^{18}O$, suggesting a gradual decrease of the oxygen content of seawater. The anoxic condition estimated from the high Mn and Fe contents is also consistent with the positive or faint negative Ce anomaly of carbonate rocks (Yang et al., 1999) and carbonate minerals (Komiya et al., 2008b) in the upper Doushantuo Formation. The combination of a high $\delta^{13}C$ and a decrease of the oxygen content of seawater suggests a high primary productivity and consumption of seawater oxygen by aerobic respiration and oxidation of reductive materials flowing in the oceans during the period, because a high $\delta^{13}C$ value indicates high primary productivity, and concomitant higher biological activity. In P-4, $\delta^{13}C_{carb}$ suddenly decreased to a nadir of −9‰. The sudden decrease in $\delta^{13}C_{carb}$ was accompanied by a high $^{87}Sr/^{86}Sr$ value and high Mn and Fe contents of carbonate rocks, evidence of high continental weathering and a low oxygen content of seawater. The decrease of the oxygen content due to remineralization of the DOC is qualitatively consistent with model calculations (Bristow and Kennedy, 2008). This line of evidence supports the idea that a higher sulfate influx due to higher continental weathering caused the remineralization of the DOC to DIC through active sulfate reduction (Fike et al., 2006), and that the remineralization and oxidative decay of the DOC and aerobic respiration consequently decreased the oxygen content of seawater. These events continued through the Shuram excursion. In the final stage, the remineralization ceased so that $\delta^{13}C$ increased, whereas Mn and Fe contents decreased. The latter indicates an increase of the oxygen content of seawater, consistent with late-stage oxidation, evident in sulfur isotope studies (Fike et al., 2006).

Finally, we summarize the events from the chemostratigraphies of the $\delta^{13}C$ and $^{87}Sr/^{86}Sr$ values and Mn and Fe contents in P-3 and P-4. The formation of mountain chains due to continental collisions increases continental weathering. The erosion of continental materials supplied more nutrients (e.g. phosphorus and calcium), and possibly promoted primary productivity. Because of the high primary productivity, the ocean temporarily became oxic, but the consumption of O_2 by respiration of the expanded biomass, oxidation of reductive materials flowing into the ocean and the oxidation of the DOC restored the ocean to a reductive condition. Extensive remineralization of the DOC through sulfate reduction and oxidative decay of the DOC shrank the excess DOC reservoir.

5.5. $^{87}Sr/^{86}Sr$ excursion against time

We now reconstruct the secular change in the $^{87}Sr/^{86}Sr$ ratio of seawater in the Ediacaran, based on geochronology and $\delta^{13}C$ values. Recently, Halverson et al. (2007) tried to reconstruct the secular change of $^{87}Sr/^{86}Sr$ in the Neoproterozoic based on compilation of $^{87}Sr/^{86}Sr$ data in Canada, Svalbard, Namibia, Oman and Australia. A remarkable difference from the previous works is that we can now obtain the $^{87}Sr/^{86}Sr$ data from a completely continuous section in one area in South China, whereas in the past the results were reconstructed from $^{87}Sr/^{86}Sr$ data with poorly constrained ages and sporadically obtained from five areas (Fig. 1).

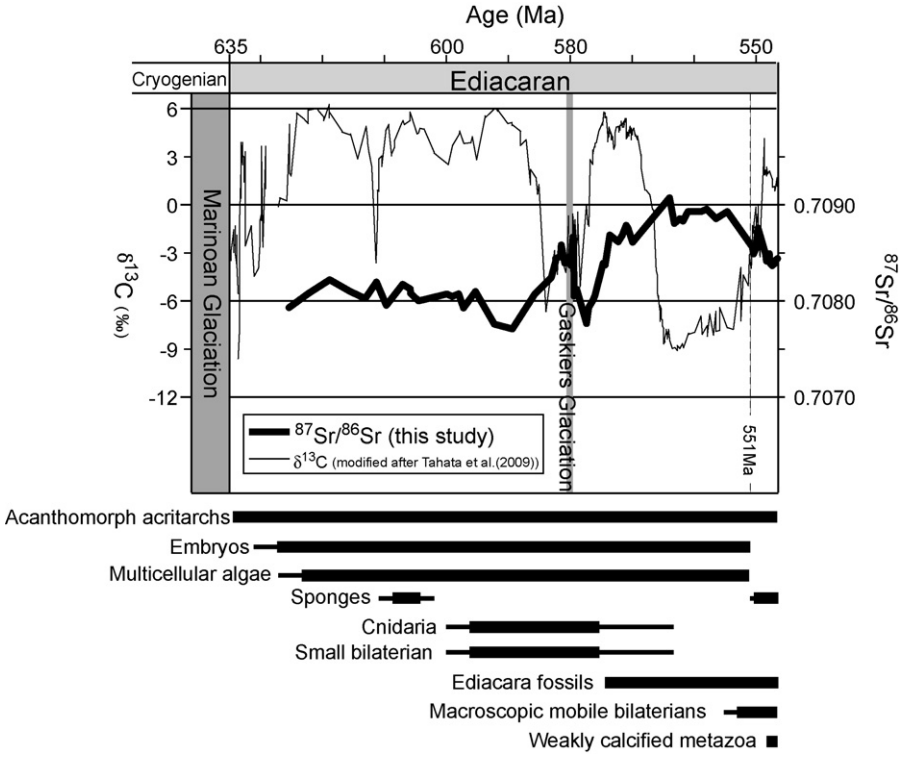

Fig. 9. Reconstructed oceanic $^{87}Sr/^{86}Sr$ and $\delta^{13}C$ changes in the Ediacaran and simplified biological evolution (modified after Li et al., 1998; Xiao et al., 2000; Brasier and Antcliffe, 2004; Fike et al., 2006). The horizontal age axis of $^{87}Sr/^{86}Sr$ and $\delta^{13}C$ are estimated based on three points at the bottom of the Doushantuo Fm (635 Ma), the Gaskiers glaciation (*ca.* 580 Ma), and the top of the Doushantuo Fm (551 Ma).

The bottom of the Doushantuo Fm is fixed at 635 Ma (Condon et al., 2005), the negative $\delta^{13}C$ anomaly in P-2 at the 580 Ma Gaskiers glaciation (Bowring et al., 2003), and the top of the Doushantuo Fm at 551 Ma (Condon et al., 2005). We evenly expanded and/or reduced the chemostratigraphies among the fixed points to reconstruct the secular change of the $^{87}Sr/^{86}Sr$ ratio of seawater (Fig. 9). The results show that the oceanic $^{87}Sr/^{86}Sr$ ratio temporarily increased and decreased at the Gaskiers glaciation, and then rose after *ca.* 575 Ma, in contrast to Halverson and Hurtgen (2007) and Halverson et al. (2007), because these earlier workers assumed that the Shuram excursion was caused by the Gaskiers glaciation and because the timing of the Gaskiers glaciation was not defined by their chemostratigraphy of $\delta^{13}C$. Relatively high $^{87}Sr/^{86}Sr$ ratios (>0.7077) rather than other ages might be attributed to formation of a long-term Trans-Gondwana mountain chain. $^{87}Sr/^{86}Sr$ ratios in the Ediacaran are generally higher than those in pre-Ediacaran (>635 Ma) and post-Cambrian (<490 Ma) rocks, and a Trans-Gondwana mountain chain probably existed between *ca.* 650 and 500 Ma. So, we speculate that these long-term high $^{87}Sr/^{86}Sr$ ratios during the Ediacaran to Cambrian were a result of the Trans-Gondwana mountain chain. Some periods with quite high $^{87}Sr/^{86}Sr$ values in late Ediacaran were possibly also caused by relatively short intervals of continental collisional events during the formation of the Trans-Gondwana mountain chain. The influence of continental collisions around the Mozambique and Kuunga sutures (Boger and Miller, 2004) may be preserved in large positive $^{87}Sr/^{86}Sr$ excursions in P-3 to 4 in the late Ediacaran (this work) and around the PC–C boundary (Sawaki et al., 2008), respectively.

After the Gaskiers glaciation, the Ediacara biota began to flourish from *ca.* 575 Ma (Bowring et al., 2003; Narbonne and Gehling, 2003; Xiao and Laflamme, 2008). Simultaneously, oceanic organisms possibly thrived and produced high primary productivity, evident in a positive shift of $\delta^{13}C$. The enhanced continental weathering during the Gaskiers glaciation and subsequent continental collisions led to higher essential elements such as phosphorus and calcium in seawater so higher primary productivity was achieved. In addition, the higher nutrient content in seawater possibly promoted the evolution of life, namely the emergence of the Ediacara fauna. On the other hand, oxygen in seawater was consumed by the possibly enhanced respiration of aerobic organisms including Ediacara biota and the Metazoa, as well as by the oxidation of the DOC and reductive materials flowing into the ocean. In the Shuram excursion, there was a remarkable negative shift of $\delta^{13}C$, accounted for by the remineralization and oxidation of the DOC, namely a consumption of the oxygen content of seawater. At the late stage of the Shuram excursion, namely the recovery of the $\delta^{13}C$ anomaly, the oxygen content of seawater increased again, evident in the decrease of Mn and Fe contents and a large sulfur isotope fractionation, $\Delta\delta^{34}S$ (Fike et al., 2006). The continued higher continental weathering rate and higher oxygen content, as well as the formation of shallow marine environments caused by local continental rifting (Meert and Lieberman, 2008) as a new niche for the Metazoa, possibly promoted the biological activity in the latest Ediacaran.

6. Conclusions

This work presents the first detailed $^{87}Sr/^{86}Sr$ and $\delta^{13}C$ chemostratigraphies through the Ediacaran. Analyses of drill-core samples enabled us to compare more closely $\delta^{13}C$, $\delta^{18}O$ and $^{87}Sr/^{86}Sr$ chemostratigraphies. The $^{87}Sr/^{86}Sr$ chemostratigraphy displays two major positive shifts of $^{87}Sr/^{86}Sr$ in the Ediacaran, and detailed comparison among them shows that the lower positive shift is accompanied by a negative $\delta^{13}C$ and positive $\delta^{18}O$ anomalies, whereas the upper began together with a positive $\delta^{13}C$ shift before the Shuram negative $\delta^{13}C$ excursion and then it continued through the excursion.

The chemostratigraphies of $\delta^{13}C$, $\delta^{18}O$ and $^{87}Sr/^{86}Sr$ were separated into four sections from P-1 to P-4 in ascending order based on their $^{87}Sr/^{86}Sr$ variations. In P-1, there were negative correlations between $\delta^{13}C$ and $\delta^{18}O$. P-2 is defined by a positive $^{87}Sr/^{86}Sr$ excursion, accompanied by negative $\delta^{13}C$ and positive $\delta^{18}O$ anomalies. Higher $^{87}Sr/^{86}Sr$ values indicate an enhancement of continental weathering, whereas a positive $\delta^{18}O$ excursion suggests global cooling. Global regression due to global cooling enhances oxidative decay of exposed marine organic sediments, and continental weathering. The latter caused remineralization of the DOC through active sulfate reduction owing to high sulfate influx from continents and oxidation of the DOC through increased primary productivity due to high continental nutrient influx. The 580 Ma Gaskiers glaciation accounts for a close correlation between positive $^{87}Sr/^{86}Sr$, negative $\delta^{13}C$ and positive $\delta^{18}O$ excursions. In P-3, the $^{87}Sr/^{86}Sr$ value increased together with high $\delta^{13}C$ values, and an increase in Mn and Fe contents. The positive correlation of $\delta^{13}C$ and $^{87}Sr/^{86}Sr$ values is consistent with an enhanced continental weathering rate due to continental collisions between East Africa, India and Madagascar from 590 to 550 Ma (Boger and Miller, 2004; Squire et al., 2006). The increase of $^{87}Sr/^{86}Sr$ and $\delta^{13}C$ indicates higher primary activity due to the enhancement of continental weathering and consequent higher nutrient contents in seawater, and the accompanied decrease in Mn and Fe contents suggests oxidation possibly due to the high primary productivity and subsequent increase in Mn and Fe contents implies a decrease in the oxygen content of seawater due to more active aerobic respiration and reductive materials flowing into the oceans during the period.

P-4 is defined by a large $\delta^{13}C$ negative anomaly, the so-called Shuram excursion, and it possesses higher $^{87}Sr/^{86}Sr$ values and a transition from an increase to a decrease in Mn and Fe contents. The higher $^{87}Sr/^{86}Sr$ values are the first compelling evidence for enhanced continental weathering, which caused the large $\delta^{13}C$ negative anomaly through the remineralization of the DOC by more active sulfate reduction due to a higher sulfate influx. Higher Mn and Fe contents in the early and middle stages of the Shuram excursion suggest a decline in the oxygen content of seawater due to oxidative decay of the DOC, whereas during the late stage, the decrease in Mn and Fe contents is consistent with oceanic oxygenation (Fike et al., 2006).

The emergence of Ediacara biota after the Gaskiers glaciation and the prosperity in the latest Ediacaran suggests that enhanced continental weathering and the consequent higher influxes of nutrients played an important role in biological evolution.

Acknowledgements

We appreciate Prof. P.F. Hoffman and an anonymous reviewer for constructive reviews and comments. We thank Yoko Ohtsuka, Hiroshi Matsuo and Hitomi Tokimori for technical advice (ICP-OES) at the Center for Advanced Materials Analysis in the Tokyo Institute of Technology. We also thank Dr. Takahiro Wakabayashi for assistance (ICP-MS) in the acquisition of analytical data. This work was partly supported by grants for "Secular variation of seawater composition (No. 16740284)", and for "Coevolution of surface environment and solid earth from the Neoproterozoic Snowball Earth to Cambrian explosion events (No. 18740318)" from the Ministry of Education, Culture, Sports, Science and Technology, Japan.

Appendix A. Supplementary data

Supplementary data associated with this article can be found, in the online version, at doi:10.1016/j.precamres.2009.10.006.

References

Amthor, J.E., Grotzinger, S., Schröder, S.A., Bowring, J., Ramezani, M., Martin, M., Matter, A., 2003. Extinction of Cloudina and Namacalathus at the Precambrian–Cambrian boundary in Oman. Geology 31, 431–434.

Asmerom, Y., Jacobsen, S.B., Knoll, A.H., Butterfield, N.J., Swett, K., 1991. Strontium isotopic variations of Neoproterozoic seawater: implications for crustal evolution. Geochimica et Cosmochimica Acta 55, 2883–2894.

Babcock, L.E., Peng, S., 2007. Cambrian chronostratigraphy: current state and future plans. Palaeogeography, Palaeoclimatology, Palaeoecology 254, 62–66.

Barfod, G.H., Albaréde, F., Knoll, A.H., Xiao, S., Télouk, P., Frei, R., Baker, J., 2002. New Lu–Hf and Pb–Pb age constraints on the earliest animal fossils. Earth and Planetary Science Letters 201, 203–212.

Banner, J.L., Hanson, G.N., 1990. Calculation of simultaneous isotopic and trace element variations during water-rock interaction with applications to carbonate diagenesis. Geochimica et Cosmochimica Acta 54, 3123–3137.

Bengtson, S., Budd, G., 2004. Comment on "Small bilaterian fossils from 40 to 55 Million Years before the Cambrian". Science 306, 1291a.

Blum, J.D., Erel, Y., Brown, K., 1993. $^{87}Sr/^{86}Sr$ ratios of Sierra Nevada stream waters: implications for relative mineral weathering rates. Geochimica et Cosmochimica Acta 57, 5019–5025.

Blum, J.D., Erel, Y., 1995. A silicate weathering mechanism linking increases in marine $^{87}Sr/^{86}Sr$ with global glaciation. Nature 373, 415–418.

Boger, S.D., Miller, J.M., 2004. Terminal suturing of Gondwana and the onset of the Ross-Delamerian Orogeny: the cause and effect of an Early Cambrian reconfiguration of plate motions. Earth and Planetary Science Letters 219, 35–48.

Bowring, S.A., Myrow, P., Landing, E., Ramenzani, J., 2003. NASA Astrobiology Unit, General Meeting 2003, Abstract 13045, http://nai.arc.nasa.gov/institute/general_meeting_2003/Abstract Book.pdf.

Brand, U., Veizer, J., 1980. Chemical diagenesis of a multicomponent carbonate system. 1. Trace elements. Journal of Sedimentary Petrology 50, 1219–1236.

Brand, U., Veizer, J., 1981. Chemical diagenesis of a multicomponent carbonate system. 2. Stable isotopes. Journal of Sedimentary Petrology 51, 987–997.

Brasier, M., Antcliffe, J., 2004. Paleobiology: decoding the Ediacaran Enigma. Science 305, 1115–1117.

Brasier, M.D., Shields, G., Kuleshov, V.N., Zhegallo, E.A., 1996. Integrated chemo- and biostratigraphic calibration of early animal evolution: Neoproterozoic-early Cambrian of Southwest Mongolia. Geological Magazine 133, 445–485.

Bristow, T.F., Kennedy, M.J., 2008. Carbon isotope excursions and the oxidant budget of the Ediacaran atmosphere and ocean. Geology 36, 863–866.

Broecker, W.S., 1982. Ocean chemistry during glacial time. Geochimica et Cosmochimica Acta 46, 1689–1705.

Burns, S.J., Haudenschild, U., Matter, A., 1994. The strontium isotopic composition of carbonates from the late Precambrian (~560–540 Ma) Huqf Group of Oman. Chemical Geology 111, 269–282.

Calver, C.R., 2000. Isotope stratigraphy of the Ediacaran Neoproterozoic (III) of the Adelaide Rift Complex, Australia, and the overprint of water column stratification. Precambrian Research 100, 121–150.

Canfield, D.E., Poulton, S.W., Narbonne, G.M., 2007. Late Neoproterozoic deep ocean oxygenation and the rise of animal life. Science 315, 92–95.

Canfield, D.E., Poulton, S.W., Knoll, A.H., Narbonne, G.M., Ross, G., Goldberg, T., Strauss, H., 2008. Ferruginous conditions dominated later Neoproterozoic deep-water chemistry. Science 321, 949–952.

Chen, P., 1987. The Sinian system. In: Wang, X. (Ed.), Stratigraphic Excursion Guidebook in the Yangtze Gorge Area. Yichang Institute of Geology and Mineral Resources, Chinese Academy of Geological Sciences, Geological Publishing House, Beijing, China, pp. 2–7.

Chen, J.-Y., Oliveri, P., Li, C.-W., Zhou, G.-Q., Gao, F., Hagadorn, J.W., Peterson, K.J., Davidson, E.H., 2000. Special feature: Precambrian animal diversity: putative phosphatized embryos from the Doushantuo Formation of China. Proceedings of the National Academy of Sciences of the United States of America 97, 4457–4462.

Chen, J.Y., Oliveri, P., Gao, F., Dornbos, S.Q., Li, C.W., Bottjer, D.J., Davidson, E.H., 2002. Precambrian animal life: probable developmental and adult cnidarian forms from S. W. China. Developmental Biology 248, 182–196.

Chen, J.Y., Bottjer, D.J., Oliveri, P., Dornbos, S.Q., Gao, F., Ruffins, S., Chi, H., Li, C.W., Davidson, E.H., 2004. Small bilaterian fossils from 40 to 55 million, years before the Cambrian. Science 305, 218–222.

Chen, M., Chen, Y., Qian, Y., 1981. Some tubular fossils from Sinian–Cambrian boundary sequence, Yangtze Gorges, Bulletin of Tianjin Institute of Geology and Mineral Resources 3. Tianjin Institute of Geology and Mineral Resources, 117–124.

Condon, D., Zhu, M., Bowring, S., Wang, W., Yang, A., Jin, Y., 2005. U–Pb ages from the Neoproterozoic Doushantuo Formation, China. Science 308, 95–98.

Derry, L.A., Keto, L.S., Jacobsen, S.B., Knoll, A.H., Swett, K., 1989. Sr isotopic variations in Upper Proterozoic carbonates from Svalbard and East Greenland. Geochimica et Cosmochimica Acta 53, 2331–2339.

Dickens, G.R., O'Neil, J.R., Rea, D.K., Owen, R.M., 1995. Dissociation of oceanic methane hydrate as a cause of the carbon isotope excursion at the end of the Paleocene. Paleoceanography 10, 965–971.

Ding, L., Li, Y., Chen, H., 1992. Discovery of Micrhystridium Regulare from Sinian–Cambrian boundary strata in Yichang, Hubei, and its stratigraphic significance. Acta Micropaleontologica Sinica 9, 303–309.

Dong, L., Xiao, S.H., Shen, B., Zhou, C., Li, G., Yao, J., 2009. Basal Cambrian microfossils from the Yangtze Gorges area (South China) and the Aksu area (Tarim block, northwestern China). Journal of Paleontology 83, 30–44.

Elderfield, H., 1986. Strontium isotope stratigraphy. Palaeogeography, Palaeoclimatology, Palaeoecology 57, 71–90.

Fietzke, J., Eisenhauer, A., 2006. Determination of temperature-dependent stable strontium isotope ($^{88}Sr/^{86}Sr$) fractionation via bracketing standard MC-ICP-MS. Geochemistry, Geophysics, Geosystems 7, Q08009, doi:10.1029/2006GC001243.

Fike, D.A., Grotzinger, J.P., Pratt, L.M., Summons, R.E., 2006. Oxidation of the Ediacaran ocean. Nature 444, 744–747.

Foden, J., Barovich, K., Jane, M., O'Halloran, G., 2001. Sr-isotopic evidence for Late Neoproterozoic rifting in the Adelaide geosyncline at 586 Ma: implications for a Cu ore forming fluid flux. Precambrian Research 106, 291–308.

Glaessner, M.F., Wade, M., 1996. The Late Precambrian fossils from Ediacara, South Australia. Palaeontology 9, 599–628.

Grotzinger, J.P., Bowring, S.A., Saylor, B.Z., Kaufman, A.J., 1995. Biostratigraphic and geochronologic constraints on early animal evolution. Science 270, 598604.

Halicz, L., Segal, I., Fruchter, N., Stein, M., Lazar, B., 2008. Strontium stable isotopes fractionate in the soil environments? Earth and Planetary Science Letters 272, 406–411.

Halverson, G.P., Hoffman, P.F., Schrag, D.P., Maloof, A.C., Rice, A.H.N., 2005. Toward a Neoproterozoic composite carbon-isotope record. Geological Society of America Bulletin 117, 1181–1207.

Halverson, G.P., 2006. A Neoproterozoic chronology. Neoproterozoic Geobiology and Paleobiology, 231–271.

Halverson, G.P., Dudás, F.Ö., Maloof, A.C., Bowring, S.A., 2007. Evolution of the $^{87}Sr/^{86}Sr$ composition of Neoproterozoic seawater. Palaeogeography, Palaeoclimatology, Palaeoecology 256, 103–129.

Halverson, G.P., Hurtgen, M.T., 2007. Ediacaran growth of the marine sulfate reservoir. Earth and Planetary Science Letters 263, 32–44.

Higgins, J.A., Schrag, D.P., 2006. Beyond methane: towards a theory for the Paleocene–Eocene thermal maximum. Earth and Planetary Science Letters 245, 523–537.

Hirata, T., Nesbitt, R.W., 1995. U–Pb isotope geochronology of zircon: evaluation of the laser probe-inductively coupled plasma mass spectrometry technique. Geochimica et Cosmochimica Acta 59, 2491–2500.

Hirata, T., Shimizu, H., Akagi, T., Sawatari, H., Masuda, A., 1988. Precise determination of rare earth elements in geological standard rocks by inductively coupled plasma source mass spectrometry. Analytical Sciences 4, 637–643.

Hodell, D.A., Mead, G.A., Mueller, P.A., 1990. Variation in the strontium isotopic composition of seawater (8 Ma to present): implications for chemical weathering rates and dissolved fluxes to the oceans. Chemical Geology 80, 291–307.

Hoffman, P.F., Kaufman, A.J., Halverson, G.P., Schrag, D.P., 1998. A Neoproterozoic Snowball Earth. Science 281, 1342–1346.

Hoffman, P.F., Schrag, D.P., 2002. The Snowball Earth hypothesis: testing the limits of global change (review article). Terra Nova 14, 129–155.

Hurtgen, M.T., Arthur, M.A., Halverson, G.P., 2005. Neoproterozoic sulfur isotopes, the evolution of microbial sulfur species, and the burial efficiency of sulfide as sedimentary pyrite. Geology 33, 41–44.

Ishikawa, T., Ishikawa, T., Ueno, Y., Komiya, T., Sawaki, Y., Shu, D., Li, Y., Maruyama, S., Han, J., 2008. C-isotope chemostratigraphy of a PC/C boundary section, Three Gorge area, South China: basal-Tommotian regression and Cambrian Explosion. Gondwana Research 14, 193–208.

Jacobsen, S.B., Kaufman, A.J., 1999. The Sr, C and O isotopic evolution of Neoproterozoic seawater. Chemical Geology 161, 37–57.

Jiang, G., Christie-Blick, N., Kaufman, A.J., Banerjee, D.M., Rai, V., 2002. Sequence stratigraphy of the Neoproterozoic Infra Krol Formation and Krol Group, Lesser Himalaya, India. Journal of Sedimentary Research 72, 524–542.

Jiang, G.-Q., Kennedy, M.J., Christie-Blick, N., 2003. Stable isotopic evidence for methane seeps in Neoproterozoic. Nature 426, 822–826.

Jiang, G., Kaufman, A.J., Christie-Blick, N., Zhang, S., Wu, H., 2007. Carbon isotope variability across the Ediacaran Yangtze platform in South China: Implications for a large surface-to-deep ocean $\delta^{13}C$ gradient. Earth and Planetary Science Letters 261, 303–320.

Jiang, G.-Q., Zhang, S.H., Shi, X.Y., Wang, X.-Q., 2008. Chemocline instability and isotope variations of the Ediacaran Doushantuo basin in South China. Science in China Series D: Earth Sciences 51, 1560–1569.

Kaufman, A.J., Jacobsen, S.B., Knoll, A.H., 1993. The Vendian record of Sr and C isotopic variations in seawater: implications for tectonics and paleoclimate. Earth and Planetary Science Letters 120, 409–430.

Kaufman, A.J., Knoll, A.H., 1995. Neoproterozoic variations in the C-isotope composition of seawater: stratigraphic and biogeochemical implications. Precambrian Research 73, 27–49.

Kaufman, A.J., Knoll, A.H., Narbonne, G.M., 1997. Isotopes, ice ages, and terminal Proterozoic earth history. Proceedings of the National Academy of Sciences of the United States of America 94, 6600–6605.

Kaufman, A.J., Jiang, G., Christie-Blick, N., Banerjee, D.M., Rai, V., 2006. Stable isotope record of the terminal Neoproterozoic Krol platform in the Lesser Himalayas of northern India. Precambrian Research 147, 156–185.

Kaufman, A.J., Corsetti, F.A., Varni, M.A., 2007. The effect of rising atmospheric oxygen on carbon and sulfur isotope anomalies in the Neoproterozoic Johnnie Formation, Death Valley, USA. Chemical Geology 237, 47–63.

Kennedy, M.J., Runnegar, B., Prave, A.R., Hoffmann, K.H., Arthur, M.A., 1998. Two or four Neoproterozoic glaciations? Geology 26, 1059–1063.

Knoll, A.H., Bambach, R.K., Canfield, D.E., Grotzinger, J.P., 1996. Comparative earth history and late Permian mass extinction. Science 273, 452–457.

Komiya, T., Suga, A., Ohno, T., Han, J., Guo, J., Yamamoto, S., Hirata, T., Li, Y., 2008a. Ca isotopic compositions of dolomite, phosphorite and the oldest animal embryo

fossils from the Neoproterozoic in Weng'an, South China. Gondwana Research 14, 209–218.
Komiya, T., Hirata, T., Kitajima, K., Yamamoto, S., Shibuya, T., Sawaki, Y., Ishikawa, T., Shu, D., Li, Y., Han, J., 2008b. Evolution of the composition of seawater through geologic time, and its influence on the evolution of life. Gondwana Research 14, 159–174.
Kump, L.R., Arthur, M.A., Patzkowsky, M.E., Gibbs, M.T., Pinkus, D.S., Sheehan, P.M., 1999. A weathering hypothesis for glaciation at high atmospheric pCO_2 during the Late Ordovician. Palaeogeography, Palaeoclimatology, Palaeoecology 152, 173–187.
Kuznetsov, A., Semikhatov, M., Gorokhov, I., Melnikov, N., Konstantinova, G., Kutyavin, E., 2003. Sr isotopic composition in carbonates of the Karatau Group, southern Urals, and standard curve of $^{87}Sr/^{86}Sr$ variations in the Late Riphean ocean. Stratigraphy and Geological Correlation 11, 415–449.
Lee, L.S., Chao, Y.T., 1924. Geology of the Gorge district of the Yangtze (from Ichang to Tzekuei) with special reference to the development of the Gorges. Bulletin of the Geological Society of China 3, 351–391.
Le Guerroué, E., Allen, P.A., Cozzi, A., Etienne, J.L., Fanning, M., 2006. 50 Myr recovery from the largest negative $\delta^{13}C$ excursion in the Ediacaran ocean. Terra Nova 18, 147–153.
Lemarchand, D., Wasserburg, G.J., Papanastassiou, D.A., 2004. Rate-controlled calcium isotope fractionation in synthetic calcite. Geochimica et Cosmochimica Acta 68, 4665–4678.
Li, C.-W., Chen, J.-Y., Hua, T.-E., 1998. Precambrian sponges with cellular structures. Science 279, 879–882.
Li, G., Chen, J., Ji, J., Liu, L., Yang, J., Sheng, X., 2007. Global cooling forced increase in marine strontium isotopic ratios: importance of mica weathering and a kinetic approach. Earth and Planetary Science Letters 254, 303–312.
Liu, H.Y., Sha, Q.A., 1963. Some problems on the Sinian system of the Yi-Chang Gorge districts of the Yangtze River. Scientia Geologica Sinica 4, 177–188.
Liu, P.J., Yin, C.Y., Gao, L.Z., Tang, F., Chen, S.M., 2009. New material of microfossils from the Ediacaran Doushantuo Formation in the Zhangcunping area, Yichang, Hubei Province and its zircon SHRIMP U–Pb age. Chinese Science Bulletin 54, 1058–1064.
McFadden, K.A., Huang, J., Chu, X., Jiang, G., Kaufman, A.J., Zhou, C., Yuan, X., Xiao, S., 2008. Pulsed oxidation and biological evolution in the Ediacaran Doushantuo Formation. Proceedings of the National Academy of Sciences of the United States of America 105, 3197–3202.
Meert, J.G., Lieberman, B.S., 2008. The Neoproterozoic assembly of Gondwana and its relationship to the Ediacaran–Cambrian radiation. Gondwana Research 14, 5–21.
Melezhik, V.A., Gorokhov, I.M., Kuznetsov, A.B., Fallick, A.E., 2001. Chemostratigraphy of Neoproterozoic carbonates: implications for 'blind dating'. Terra Nova 13, 1–11.
Melezhik, V.A., Pokrovsky, B.G., Fallick, A.E., Kuznetsov, A.B., Bujakaite, M.I., 2009. Constraints on $^{87}Sr/^{86}Sr$ of Late Ediacaran seawater: insight from Siberian high-Sr limestones. Journal of the Geological Society, London 166, 183–191.
Myrow, P.M., Kaufman, A.J., 1999. A newly discovered cap carbonate above Varanger-age glacial deposits in Newfoundland, Canada. Journal of Sedimentary Research 69, 784–793.
Narbonne, G.M., Gehling, J.M., 2003. Life after snowball: the oldest complex Ediacaran fossils. Geology 31, 27–30.
Narbonne, G.M., Kaufman, A.J., Knoll, A.H., 1994. Integrated chemostratigraphy and biostratigraphy of the Windermere Supergroup, northwestern Canada: implications for Neoproterozoic correlations and the early evolution of animals. Geological Society of America, Bulletin 106, 1281–1292.
Nier, A.O., 1938. The isotopic constitution of strontium, barium, bismuth, thallium, and mercury. Physical Review 5, 275–278.
Ohno, T., Hirata, T., 2006. Stable isotope geochemistry of strontium using MC-ICP-MS. Geochimica et Cosmochimica Acta 70, A453.
Ohno, T., Komiya, T., Ueno, Y., Hirata, T., Maruyama, S., 2008. Determination of $^{88}Sr/^{86}Sr$ mass-dependent isotopic fractionation and radiogenic isotope variation of $^{87}Sr/^{86}Sr$ in the Neoproterozoic Doushantuo Formation. Gondwana Research 14, 126–133.
Palmer, M.R., Edmond, J.M., 1989. The strontium isotope budget of the modern ocean. Earth and Planetary Science Letters 92, 11–26.
Pelechaty, S.M., 1998. Integrated chronostratigraphy of the Vendian System of Siberia: implications for a global stratigraphy. Journal of the Geological Society, London 155, 957–973.
Peltier, W.R., Liu, Y., Crowley, J.W., 2007. Snowball Earth prevention by dissolved organic carbon remineralization. Nature 450, 813–818.
Pokrovsky, B.G., Melezhik, V.A., Bujakaite, M.I., 2006. Carbon, oxygen, strontium and sulfur isotopic compositions in Late Precambrian rocks of the Patom complex, central Siberia: communication. 1. Results, isotope stratigraphy and dating problems. Lithology and Mineral Resources 41, 450–474.
Richter, F.M., Rowley, D.B., Depaolo, D.J., 1992. Sr isotope evolution of seawater: the role of tectonics. Earth and Planetary Science Letters 109, 11–23.
Richter, F.M., Turekian, K.K., 1993. Simple models for the geochemical response of the ocean to climatic and tectonic forcing. Earth and Planetary Science Letters 119, 121–131.
Rothman, D.H., Hayes, J.M., Summons, R.E., 2003. Dynamics of the Neoproterozoic carbon cycle. Proceedings of the National Academy of Sciences of the United States of America 100, 8124–8129.
Rüggeberg, A., Fietzke, J., Liebetrau, V., Eisenhauer, A., Dullo, W.-C., Freiwald, A., 2008. Stable strontium isotopes ($\delta^{88}/^{86}Sr$) in cold-water corals—a new proxy for reconstruction of intermediate ocean water temperatures. Earth and Planetary Science Letters 269, 570–575.
Russell, W.A., Papanastassiou, D.A., Tombrello, T.A., 1978. Ca isotope fractionation on the Earth and other solar system materials. Geochimica et Cosmochimica Acta 42, 1075–1090.
Saylor, B.Z., Kaufman, A.J., Grotzinger, J.P., Urban, F., 1998. A composite reference section for terminal Proterozoic strata of southern Namibia. Journal of Sedimentary Research 68, 1223–1235.
Sawaki, Y., Ohno, T., Fukushi, Y., Komiya, T., Ishikawa, T., Hirata, T., Maruyama, S., 2008. Sr isotope excursion across the Precambrian–Cambrian boundary in the Three Gorges area, South China. Gondwana Research 14, 134–147.
Shields, G., 1999. Working towards a new stratigraphic calibration scheme for the Neoproterozoic–Cambrian. Eclogae Geologicae Helvetiae 92, 221–233.
Shields, G.A., 2007. A normalized seawater strontium isotope curve: possible implications for Neoproterozoic–Cambrian weathering rates and the further oxygenation of the Earth. eEarth 2, 35–42.
Shields, G.A., Veizer, J., 2002. Precambrian marine carbonate isotope database: version 1.1. Geochemistry, Geophysics, Geosystems 3, doi:10.1029/2001GC000266.
Sprigg, R.C., 1947. Early Cambrian jellyfishes from the Flinders Ranges, South Australia. Transactions of the Royal Society of South Australia 71, 212–224.
Squire, R.J., Campbell, I.H., Allen, C.M., Wilson, C.J.L., 2006. Did the Transgondwanan Supermountain trigger the explosive radiation of animals on Earth? Earth and Planetary Science Letters 250, 116–133.
Steiner, M., Mehl, D., Reitner, J., Erdtmann, B.D., 1993. Oldest entirely preserved sponges and other fossils from the lowermost Cambrian and a new facies reconstruction of the Yangtze Platform (China). Berliner Geowissenschaftliche Abhandlungen 9, 293–329.
Sun, W., 1986. Late Precambrian pennatulids (sea pens) from the eastern Yangtze Gorge, China: Paracharnia gen. nov. Precambrian Research 31, 361–375.
Tahata, M., Ueno, Y., Ishikawa, T., Sawaki, Y., Murakami, K., Yoshida, N., Komiya, T., Maruyama, S., submitted for publication. High-resolution carbon isotope analysis of Ediacaran carbonate rock: decoding environmental changes after Marinoan glaciation.
Vernhet, E., 2007. Paleobathymetric influence on the development of the late Ediacaran Yangtze platform (Hubei, Hunan, and Guizhou provinces, China). Sedimentary Geology 197, 29–46.
Walter, M.R., Veevers, J.J.V., Calver, C.R., Gorjan, P., Hill, A.C., 2000. Dating the 840–544 Ma Neoproterozoic interval by isotopes of strontium, carbon, and sulfur in seawater, and some interpretative models. Precambrian Research 100, 371–433.
Wang, W., Matsumoto, R., Wang, H., Ohde, S., Kano, A., Mu, X., 2002. Isotopic, chemostratigraphy of the upper Sinian in Three Gorges area. Acta Micropalaeontologica Sinica 19, 382–388.
Wang, Z., Yin, C., Gao, L., Liu, Y., 2002. Chemostratigraphic characteristics and correlation of the Sinian stratotype in the eastern Yangtze Gorges area, Yichang, Hubei Province. Geological Review 48, 408–415 (in Chinese with English abstract).
Xiao, S., Zhang, Y., Knoll, A.H., 1998. Three-dimensional preservation of algae and animal embryos in a Neoproterozoic phosphorite. Nature 391, 554–558.
Xiao, S.H., Yuan, X.L., Knoll, A.H., 2000. Eumetazoan fossils in terminal Proterozoic phosphorites? Proceedings of the National Academy of Sciences of the United States of America 97, 13684–13689.
Xiao, S.H., Yuan, X.L., Steiner, M., Knoll, A.H., 2002. Macroscopic carbonaceous compressions in a terminal Proterozoic shale: a systematic reassessment of the Miaohe biota, south China. Journal of Paleontology 76, 347–376.
Xiao, S.H, Shen, B., Zhou, C., Xie, G., Yuan, X., 2005. A uniquely preserved Ediacaran fossil with direct evidence for a quilted body plan. Proceedings of the National Academy of Sciences of the United States of America 102, 10227–10232.
Xiao, S.H., Laflamme, M., 2008. On the eve of animal radiation: phylogeny, ecology and evolution of the Ediacara biota. Trends in Edology and Evolution 24, 31–40.
Yang, J., Sun, W., Wang, Z., Xue, Y., Tao, X., 1999. Variations in Sr and C isotopes and Ce anomalies in successions from China: evidence for the oxygenation of Neoproterozoic seawater? Precambrian Research 93, 215–233.
Yao, J., Xiao, S.H., Yin, L., Li, G., Yuan, X., 2005. Basal Cambrian microfossils from the Yurtus and Xishanblaq formations (Tarim, north-west China): systematic revision and biostratigraphic correlation of micrhystridium-like acritarchs. Palaeontology 48, 687–708.
Yin, C., Tang, F., Liu, Y., Gao, L., Liu, P., Xing, Y., Yang, Z., Wan, Y., Wang, Z., 2005. U–Pb zircon age from the base of the Ediacaran Doushantuo Formation in the Yangtze Gorges, South China: constraint on the age of Marinoan glaciation. Episodes 28, 48–49.
Yin, L., Zhu, M., Knoll, A.H., Yuan, X., Zhang, J., Hu, J., 2007. Doushantuo embryos preserved inside diapause egg cysts. Nature 446, 661–663.
Zhang, S., Jiang, G., Zhang, J., Song, B., Kennedy, M.J., Christie-Blick, N., 2005. U–Pb sensitive high-resolution ion microprobe ages from the Doushantuo Formation in south China: constraints on late Neoproterozoic glaciations. Geology 33, 473–476.
Zhao, Z., Xing, Y., Ding, Q., Liu, G., Zhao, Y., Zhang, S., Meng, X., Yin, C., Ning, B., Han, P., 1988. The Sinian System of Hubei. China University of Geosciences Press, Wuhan, 205 pp.
Zhou, C., 1997. Upper Sinian (latest Proterozoic) carbon isotope profile in Weng'an, Guizhou. Journal of Stratigraphy 21 (2), 124–129.
Zhou, C., Xiao, S., 2007. Ediacaran $\delta^{13}C$ chemostratigraphy of South China. Chemical Geology 237, 89–108.
Zhou, J.-C., Wang, X.-L., Qiu, J.-S., Gao, J.-F., 2004. Geochemistry of Meso- and Neoproterozoic mafic-ultramafic rocks from northern Guangxi, China: Arc or plume magmatism? Geochemical Journal 38, 139–152.

Zhou, C., Xie, G., McFadden, K., Xiao, S., Yuan, X., 2007. The diversification and extinction of Doushantuo-Pertatataka acritarchs in South China: causes and biostratigraphic significance. Geological Journal 42, 229–262.
Zhu, M.Y., Zhang, J.M., Steiner, M., Yang, A.H., Li, G.X., Erdtmann, B.D., 2003. Sinian-Cambrian stratigraphic framework for-shallow- to deep-water environments of the Yangtze Platform: an integrated approach. Progress in Natural Science 13, 951–960.
Zhu, M., Zhang, J., Yang, A., 2007. Integrated Ediacaran (Sinian) chronostratigraphy of South China. Palaeogeography, Palaeoclimatology, Palaeoecology 254, 7–61.